

## Electronic Supplementary Information

### Isolation and reactivity of a gold(I) hydroxytrifluoroborate complex stabilized by anion- $\pi^+$ interactions

Jiliang Zhou, Elishua D. Litle and François P. Gabbaï\*

*Department of Chemistry, Texas A&M University, College Station, TX 77843, USA*

**This document includes:**

<b>1. Materials and Methods .....</b>	<b>S3</b>
<b>2. Syntheses and Spectroscopic Data .....</b>	<b>S3</b>
<b>3. Crystallographic Details.....</b>	<b>S27</b>
<b>4. Computational Details.....</b>	<b>S28</b>
<b>5. References.....</b>	<b>S33</b>

## 1. Materials and Methods

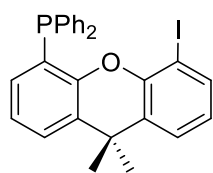
### General Remarks

Unless otherwise noted, all syntheses were carried out under an atmosphere of dry, O<sub>2</sub>-free nitrogen using standard double-manifold techniques with a rotary oil pump. A nitrogen-filled glove box was used to manipulate air-sensitive materials. Solvents were dried by refluxing under N<sub>2</sub> over CaH<sub>2</sub> (CH<sub>2</sub>Cl<sub>2</sub>) or Na (hexane) and stored under a nitrogen atmosphere over 3 Å molecular sieves. Dry deuterated chloroform (CDCl<sub>3</sub>) and dichloromethane (CD<sub>2</sub>Cl<sub>2</sub>) purchased from Cambridge Isotope Laboratories Inc. were degassed and stored over molecular sieves (3 Å) for at least two days prior to use. 4,5-Diiodo-9,9-dimethylxanthene and (tth)AuCl (tth = tetrahydrothiophene) were prepared according to literature procedures.<sup>1</sup> Commercial reagents were used without further purification unless indicated otherwise. NMR spectra were obtained on a Bruker Avance II 400 spectrometer or a Bruker Avance 500 spectrometer. <sup>1</sup>H and <sup>13</sup>C NMR chemical shifts (δ/ppm) are referenced to the residual solvent resonance of the deuterated solvent. <sup>31</sup>P, <sup>19</sup>F and <sup>11</sup>B NMR chemical shifts (δ/ppm) are referenced to H<sub>3</sub>PO<sub>4</sub>, CFCl<sub>3</sub> and BF<sub>3</sub>·OEt<sub>2</sub>, respectively. Mass spectrometry analyses were performed in-house at the Center for Mass Spectrometry. Elemental analyses were performed by Atlantic Microlab (Norcross, GA).

## 2. Syntheses and Spectroscopic Data

### 2.1 Syntheses

#### Synthesis of 4-diphenylphosphino-5-iodo-9,9-dimethylxanthene



A THF solution (60 mL) of 4,5-Diiodo-9,9-dimethylxanthene (924 mg, 2.0 mmol) was cooled to -78 °C and treated with *n*-butyllithium (2.5 M hexanes, 0.8 mL, 2.0 mmol, 1 equiv.) which was added dropwise with a syringe. After stirring for 4 h at -78 °C, the resulting mixture was treated with a THF solution (4 mL) containing Ph<sub>2</sub>PCl (441 mg, 2.0 mmol). This solution was added dropwise with a syringe. The temperature was kept at -78 °C until the end of the addition. The reaction mixture was then allowed to warm up to room temperature gradually over the course of 3 h. After stirring at room temperature for an additional 10 h, a saturated aqueous ammonium chloride solution (40 mL) was added to the reaction mixture. The aqueous phase was extracted with CH<sub>2</sub>Cl<sub>2</sub> (3 x 20 mL). The organic fractions were combined and dried over MgSO<sub>4</sub>. All volatiles were removed using a rotary evaporator, affording a colorless residue which was purified by column chromatography over silica gel using hexane/CH<sub>2</sub>Cl<sub>2</sub> (95:5, v/v). This procedure afforded 4-diphenylphosphino-5-iodo-9,9-dimethylxanthene as a colorless solid (458 mg, 44% yield). <sup>1</sup>H NMR (400.09 MHz, CDCl<sub>3</sub>): δ (ppm) 7.49 (dd, <sup>3</sup>J<sub>H-H</sub> = 8 Hz,

$^4J_{\text{H-H}} = 2$  Hz, 1H, Xanthene-*H*), 7.31 (d,  $^3J_{\text{H-H}} = 8$  Hz, 1H, Xanthene-*H*), 7.24 (m, 1H, Xanthene-*H* and 10H, Ph-*H*), 6.91 (t,  $^3J_{\text{H-H}} = 8$  Hz, 1H, Xanthene-*H*), 6.69 (t,  $^3J_{\text{H-H}} = 8$  Hz, 1H, Xanthene-*H*), 6.46 (m, 1H, Xanthene-*H*), 1.53 (s, 6H,  $\text{CMe}_2$ ).  $^{13}\text{C}\{^1\text{H}\}$  NMR (100.61 MHz,  $\text{CDCl}_3$ ):  $\delta$  (ppm) 152.1 (d,  $J_{\text{P-C}} = 17$  Hz), 149.7 (d,  $J_{\text{P-C}} = 2$  Hz), 137.8 (s), 136.7 (s), 136.6 (s), 134.5 (s), 134.3 (s), 131.9 (s), 131.2 (s), 129.7 (d,  $J_{\text{P-C}} = 1$  Hz), 128.8 (s), 128.6 (s), 128.5 (s), 126.7 (s), 126.0 (s), 125.5 (d,  $J_{\text{P-C}} = 17$  Hz), 124.8 (s), 123.9 (s), 84.8 (s), 77.4 (s), 35.0 (d,  $J_{\text{P-C}} = 1$  Hz), 32.4 (s).  $^{31}\text{P}\{^1\text{H}\}$  NMR (161.95 MHz,  $\text{CDCl}_3$ ):  $\delta$  (ppm) -14.3 (s). HRMS (ESI)  $[\text{M}+\text{H}]^+$   $\text{C}_{27}\text{H}_{23}\text{OIP}^+$  calc. 521.0526 m/z found 521.0522 m/z.

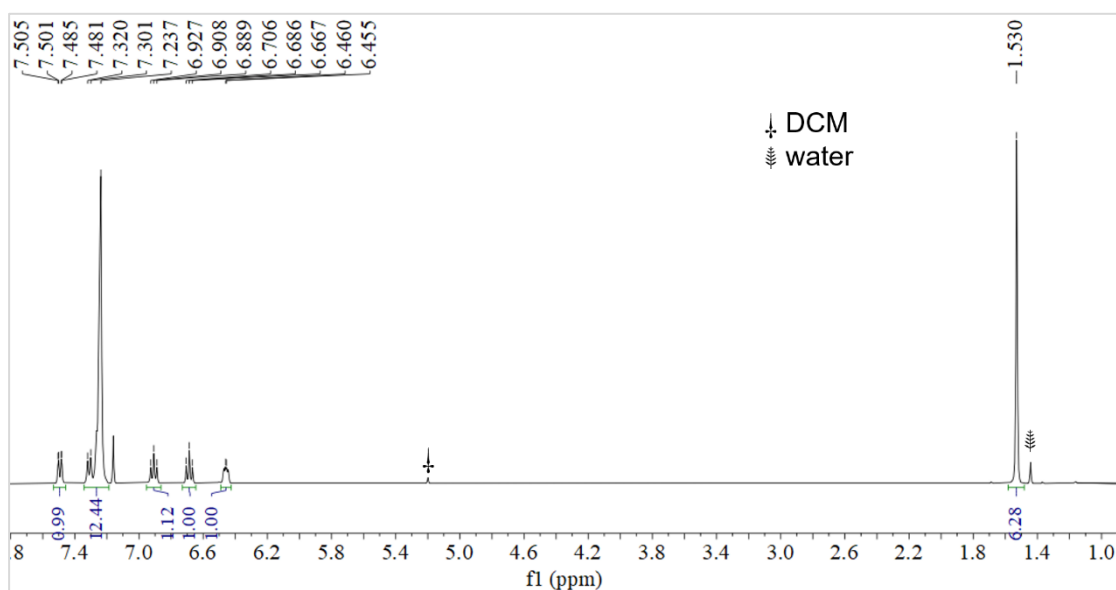


**Figure S1:**  $^1\text{H}$  NMR spectrum of 4-diphenylphosphino-5-iodo-9,9-dimethylxanthene (400.09 MHz,  $\text{CDCl}_3$ ).

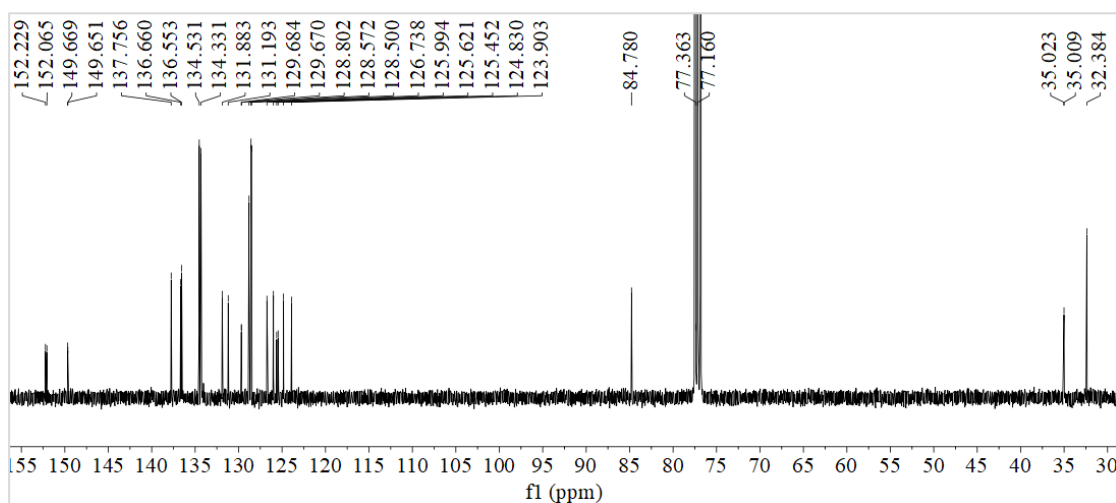


**Figure S2:**  $^{13}\text{C}\{^1\text{H}\}$  NMR spectrum of 4-diphenylphosphino-5-iodo-9,9-dimethylxanthene (100.61 MHz,  $\text{CDCl}_3$ ).

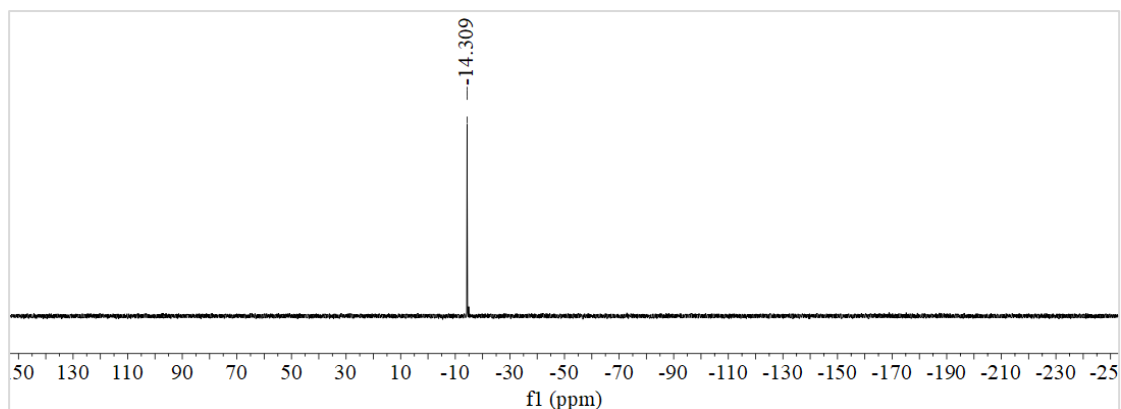
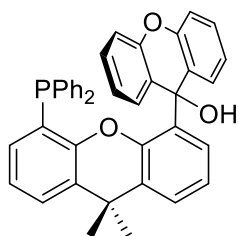


**Figure S3:**  $^{31}\text{P}\{^1\text{H}\}$  NMR spectrum of 4-diphenylphosphino-5-iodo-9,9-dimethyl-xanthene (161.95 MHz,  $\text{CDCl}_3$ ).

### Synthesis of **1**



A THF solution (40 mL) of 4-diphenylphosphino-5-iodo-9,9-dimethylxanthene (520 mg, 1.0 mmol) was cooled to  $-78\text{ }^\circ\text{C}$  and treated with *n*-butyllithium (2.5 M hexanes, 0.48 mL, 1.2 mmol, 1.2 equiv.) which was added dropwise with a syringe. After stirring for 2 h at  $-78\text{ }^\circ\text{C}$ , the resulting mixture was treated with a THF solution (4 mL) containing xanthone (196 mg, 1.0 mmol). This solution was added dropwise with a syringe. The temperature was kept at  $-78\text{ }^\circ\text{C}$  until the end of the addition. The reaction mixture was then allowed to warm up to room temperature over the course of 30 min. After stirring at room temperature for an additional 12 h, a saturated aqueous ammonium chloride solution (40 mL) was added to the reaction mixture. The aqueous phase was extracted with  $\text{CH}_2\text{Cl}_2$  (3 x 20 mL). The organic fractions were combined and dried over  $\text{MgSO}_4$ . All volatiles were removed using a rotary evaporator, affording a pale brown residue which was purified by column chromatography over silica gel using hexane/ $\text{CH}_2\text{Cl}_2$  (7:3, v/v). This procedure afforded **1** as a colorless solid (446 mg, 76% yield).  $^1\text{H}$  NMR (500.13 MHz,  $\text{DMSO}-d_6$ ):  $\delta$  (ppm) 8.08 (br, 1H, Ar-*H*), 7.64 (br, 1H, Ar-*H*), 7.42 (br, 1H, Ar-*H*), 7.36 (br, 1H, Ar-*H*), 7.21 (br, 6H, Ar-*H*), 7.03 (br, 4H, Ar-*H*), 6.85 (br, 1H, Ar-*H*), 6.78 (m, 2H, Ar-*H*), 6.66 (br, 5H, Ar-*H*), 6.32 (br, 1H, Ar-*H*), 5.79 (br, 1H, Ar-*H*), 3.30 (s, 1H, OH), 1.54 (s, 6H,  $\text{CMe}_2$ ).  $^{13}\text{C}\{^1\text{H}\}$  NMR (125.77 MHz,  $\text{DMSO}-d_6$ ):  $\delta$  (ppm) 152.5 (s), 152.4 (s), 151.3 (s), 147.0 (s), 137.7 (s), 137.6 (s), 132.6 (s), 132.5 (s), 132.3 (s), 130.7 (s), 130.6 (s), 129.9 (s), 127.9 (br), 127.8 (br), 127.7 (s), 127.6 (s), 126.9 (s), 126.2 (s), 125.6 (s), 124.0 (s), 123.9 (s), 123.2 (s), 122.3 (s), 121.9 (s), 116.3 (s), 69.0 (br), 33.9 (s), 31.4 (s).  $^{31}\text{P}\{^1\text{H}\}$  NMR (161.95 MHz,  $\text{DMSO}-d_6$ ):  $\delta$  (ppm)  $-23.4$  (s). HRMS (ESI)  $[\text{M}+\text{H}]$   $\text{C}_{40}\text{H}_{32}\text{O}_3\text{P}^+$  calc. 591.2095 m/z found 591.2079 m/z. Elemental Analysis calculated: C: 81.34, H: 5.29, found: C: 81.45, H: 5.34. IR ( $\text{cm}^{-1}$ )  $\nu(\text{O}-\text{H})$  3507 (s).

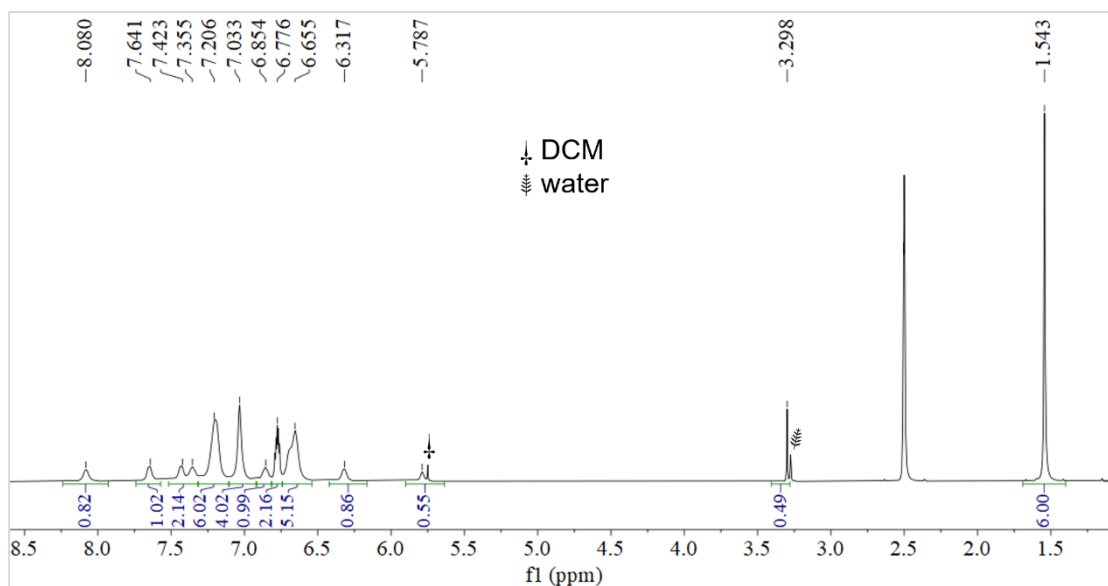


Figure S4:  $^1\text{H}$  NMR spectrum of **1** (500.13 MHz,  $\text{DMSO-}d_6$ ).

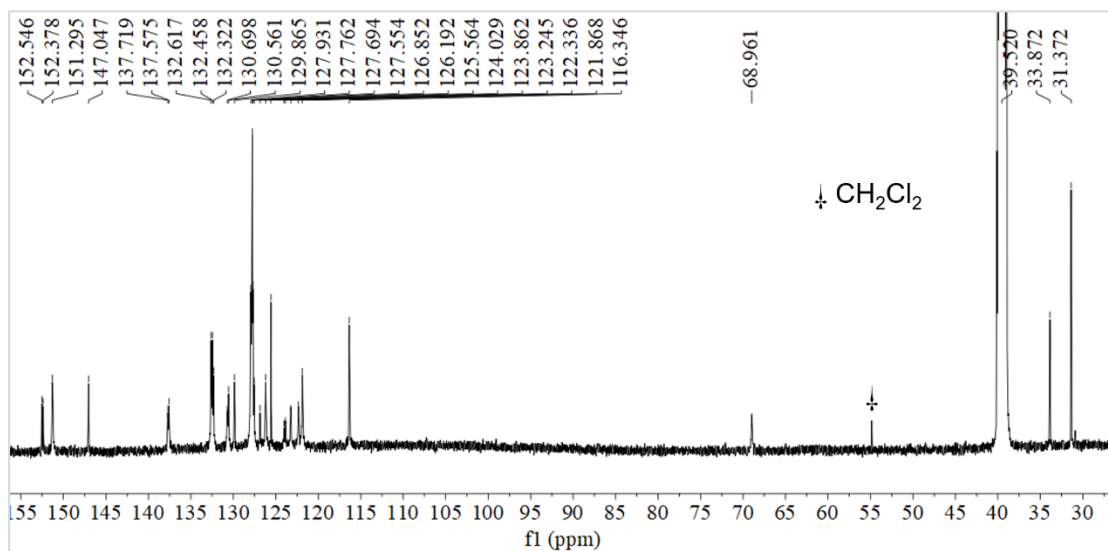


Figure S5:  $^{13}\text{C}\{^1\text{H}\}$  NMR spectrum of **1** (125.77 MHz,  $\text{DMSO-}d_6$ ).

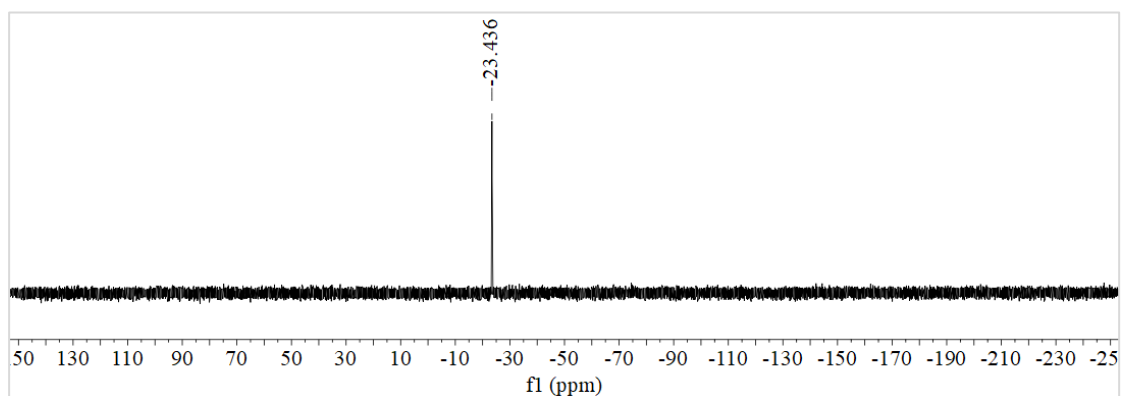
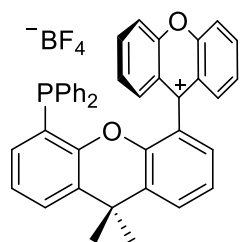
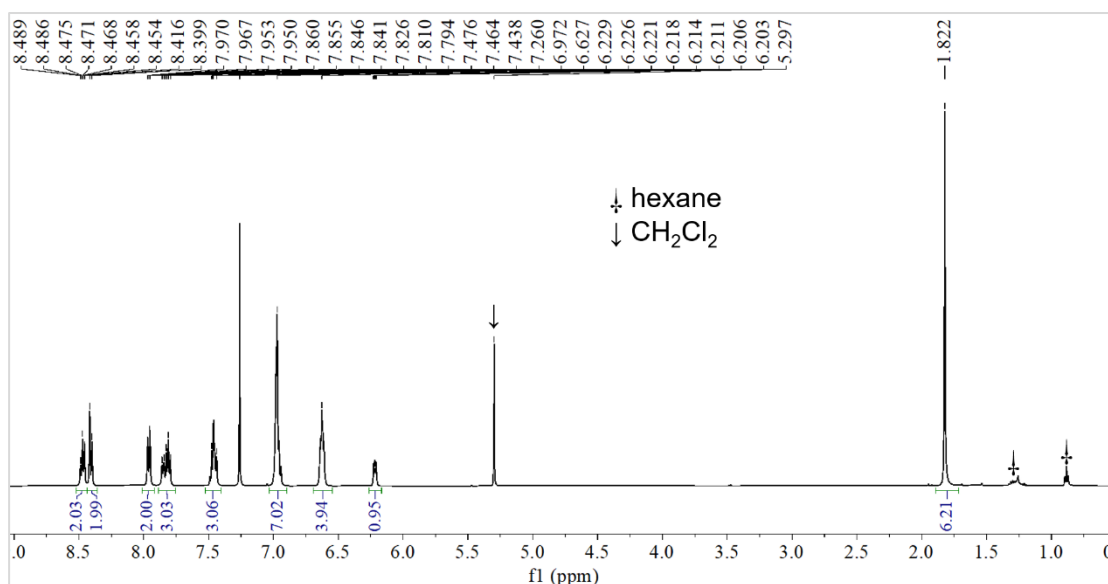


Figure S6:  $^{31}\text{P}\{^1\text{H}\}$  NMR spectrum of **1** (161.95 MHz,  $\text{DMSO-}d_6$ ).

### Synthesis of [2][BF<sub>4</sub>]



This reaction was performed under N<sub>2</sub>. Aqueous HBF<sub>4</sub> (50 wt.%, 10 μL, 7.05 mg, 0.08 mmol) was added to a CH<sub>2</sub>Cl<sub>2</sub> solution (1 mL) of **1** (47.3 mg, 0.08 mmol). The mixture was stirred at room temperature for 15 min. and combined with 6 mL of hexane under vigorous stirring. The resulting precipitate was separated by decantation and dried under vacuum to afford [2][BF<sub>4</sub>] as an orange solid (47.2 mg, 89% yield). Orange crystals of [2][BF<sub>4</sub>]·0.5(ClCH<sub>2</sub>CH<sub>2</sub>Cl) were obtained by a ClCH<sub>2</sub>CH<sub>2</sub>Cl solution upon diffusion of hexane. <sup>1</sup>H NMR (500.13 MHz, CDCl<sub>3</sub>): δ (ppm) 8.47 (ddd, <sup>3</sup>J<sub>H-H</sub> = 9 Hz, <sup>3</sup>J<sub>H-H</sub> = 7 Hz, <sup>3</sup>J<sub>H-H</sub> = 2 Hz, 2H, Xanthylum-*H*), 8.41 (d, <sup>3</sup>J<sub>H-H</sub> = 9 Hz, 2H, Xanthylum-*H*), 7.96 (dd, <sup>3</sup>J<sub>H-H</sub> = 9 Hz, <sup>3</sup>J<sub>H-H</sub> = 2 Hz, 2H, Xanthylum-*H*), 7.85 (dd, <sup>3</sup>J<sub>H-H</sub> = 7 Hz, <sup>3</sup>J<sub>H-H</sub> = 2 Hz, 1H, Xanthene-*H*), 7.81 (t, <sup>3</sup>J<sub>H-H</sub> = 9 Hz, 2H, Xanthylum-*H*), 7.46 (m, 3H, Xanthene-*H*), 6.97 (m, 1H, Xanthene-*H* and 6H, Ph-*H*), 6.63 (m, 4H, Ph-*H*), 6.21 (ddd, <sup>3</sup>J<sub>H-P</sub> = 4 Hz, <sup>3</sup>J<sub>H-H</sub> = 7 Hz, <sup>4</sup>J<sub>H-H</sub> = 2 Hz, 1H, Xanthene-*H*), 1.82 (s, 6H, CMe<sub>2</sub>). <sup>13</sup>C{<sup>1</sup>H} NMR (125.77 MHz, CDCl<sub>3</sub>): δ (ppm) 172.4 (s), 158.5 (s), 150.2 (d, *J*<sub>P-C</sub> = 16 Hz), 147.0 (s), 144.1 (s), 135.5 (s), 135.4 (s), 133.1 (s), 132.9 (s), 131.8 (s), 131.7 (s), 131.5 (s), 130.8 (s), 130.5 (s), 129.3 (s), 128.9 (s), 128.8 (s), 128.42 (s), 128.36 (s), 127.1 (s), 125.0 (d, *J*<sub>P-C</sub> = 18 Hz), 124.8 (s), 124.41 (s), 124.35 (s), 120.3 (s), 119.0 (s), 34.9 (s), 32.9 (s). <sup>31</sup>P{<sup>1</sup>H} NMR (161.95 MHz, CDCl<sub>3</sub>): δ (ppm) -14.4 (s). <sup>19</sup>F NMR (376.42 MHz, CDCl<sub>3</sub>): δ (ppm) -154.3 (s). <sup>11</sup>B{<sup>1</sup>H} NMR (128.40 MHz, CDCl<sub>3</sub>): δ (ppm) -1.4 (s). HRMS (ESI) [M<sup>+</sup>] C<sub>40</sub>H<sub>30</sub>O<sub>2</sub>P<sup>+</sup> calc. 573.1978 m/z found 573.1962 m/z.



**Figure S7:** <sup>1</sup>H NMR spectrum of [2][BF<sub>4</sub>] (500.13 MHz, CDCl<sub>3</sub>).

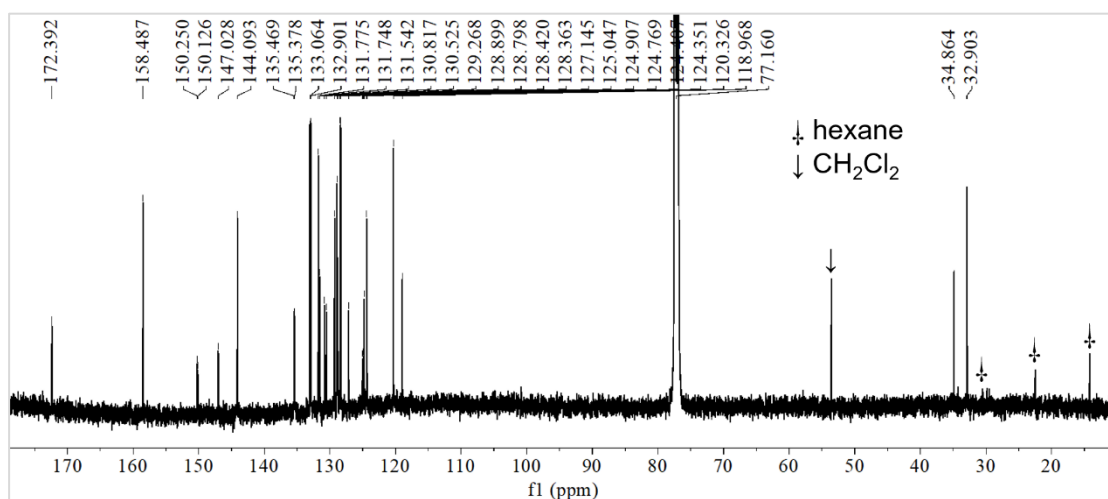


**Figure S8:**  $^{13}\text{C}\{^1\text{H}\}$  NMR spectrum of  $[\mathbf{2}][\text{BF}_4]$  (125.77 MHz,  $\text{CDCl}_3$ ).

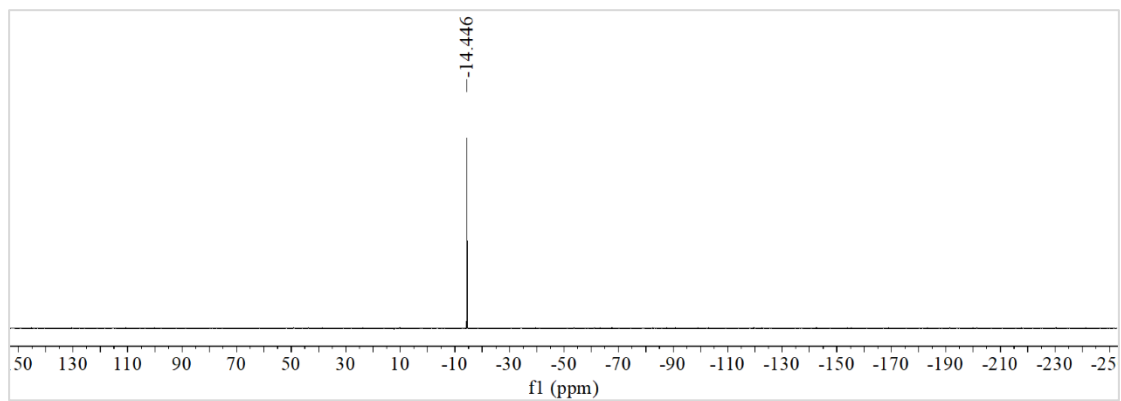


**Figure S9:**  $^{31}\text{P}\{^1\text{H}\}$  NMR spectrum of  $[\mathbf{2}][\text{BF}_4]$  (161.95 MHz,  $\text{CDCl}_3$ ).

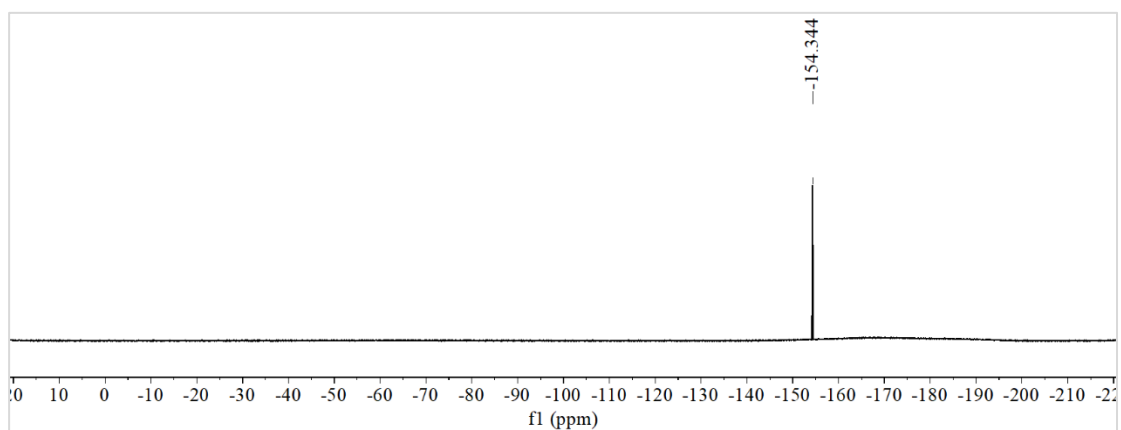


**Figure S10:**  $^{19}\text{F}$  NMR spectrum of  $[\mathbf{2}][\text{BF}_4]$  (376.42 MHz,  $\text{CDCl}_3$ ).

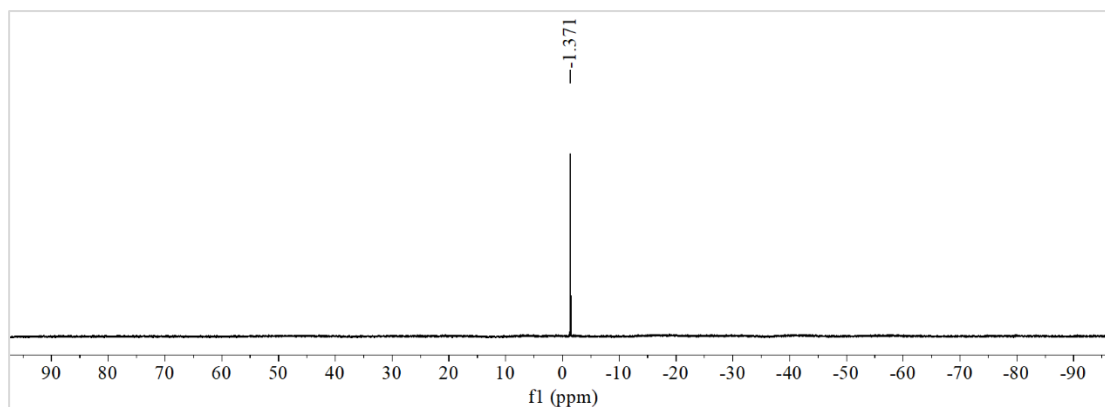
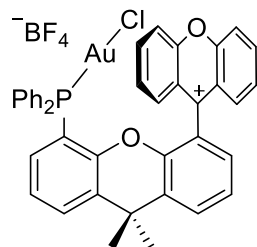


**Figure S11:**  $^{11}\text{B}\{^1\text{H}\}$  NMR spectrum of  $[\mathbf{2}][\text{BF}_4]$  (128.40 MHz,  $\text{CDCl}_3$ ).

Generation of  $[\mathbf{3}][\text{BF}_4]$  via reaction of  $[\mathbf{2}][\text{BF}_4]$  with (tht)AuCl

$[\mathbf{2}][\text{BF}_4]$  (19.8 mg, 0.03 mmol) and (tht)AuCl (9.6 mg, 0.03 mmol) were mixed in  $\sim 1$  mL of  $\text{CH}_2\text{Cl}_2$ . The resulting mixture was stirred at room temperature for 15 min. This reaction solution was combined with pentane (4 mL) under vigorous stirring to produce a fine precipitate which was separated by decantation and dried under vacuum. This procedure afforded  $[\mathbf{3}][\text{BF}_4]$  as an orange solid (26.5 mg). The solid appears to be pure by NMR spectroscopy (see below).

Synthesis of  $[\mathbf{3}][\text{BF}_4]$



$\mathbf{1}$  (59.1 mg, 0.1 mmol) and (tht)AuCl (32.1 mg, 0.1 mmol) were mixed in 2 mL of  $\text{CH}_2\text{Cl}_2$ . The resulting mixture was stirred at room temperature for 15 min and treated with  $\sim 0.1$  mL aqueous  $\text{HBF}_4$  (50%). The mixture was stirred for another 15 min. and passed through a pipette plugged with a small ball of toilet paper which we found was the best water absorbent, filtering material for this experiment. The filtrate was concentrated to  $\sim 1$  mL and combined with pentane (4 mL) under vigorous stirring to produce a fine precipitate which was separated by decantation, washed with pentane (3 mL) and dried under vacuum. This procedure afforded  $[\mathbf{3}][\text{BF}_4]$  as an orange solid (88.0 mg). The crude product appears to be pure by NMR spectroscopy (see below), but the EA results suggest the presence of minor inorganic impurities. Further purification of  $[\mathbf{3}][\text{BF}_4]$  could be achieved by recrystallization from 1,2-difluorobenzene upon layering with toluene. This procedure afforded red crystals of  $[\mathbf{3}][\text{BF}_4] \cdot (\text{toluene})$ .  $^1\text{H}$  NMR (500.13 MHz,  $\text{CDCl}_3$ ):  $\delta$  (ppm) 8.51 (m, 2H, Xanthylum-*H*), 8.36 (d,  $^3J_{\text{H-H}} = 9$  Hz, 2H, Xanthylum-*H*), 7.91 (dd,  $^3J_{\text{H-H}} = 8$  Hz,  $^3J_{\text{H-H}} = 2$  Hz, 1H, Xanthene-*H*), 7.88 (m, 4H, Xanthylum-*H*), 7.74 (d,  $^3J_{\text{H-H}} = 8$  Hz, 1H, Xanthene-*H*), 7.46 (t,  $^3J_{\text{H-H}} = 8$  Hz, 1H, Xanthene-*H*), 7.25-7.13 (m, 1H, Xanthene-*H* and 6H, Ph-*H*), 7.09 (td,  $^3J_{\text{H-H}} = 8$  Hz,  $^4J_{\text{H-H}} = 2$  Hz, 1H, Xanthene-*H*), 6.96 (d,  $^3J_{\text{H-H}} =$

7 Hz, 2H, Ph-*H*), 6.93 (d,  $^3J_{\text{H-H}} = 7$  Hz, 2H, Ph-*H*), 6.33 (ddd,  $^3J_{\text{H-P}} = 13$  Hz,  $^3J_{\text{H-H}} = 8$  Hz,  $^4J_{\text{H-H}} = 2$  Hz, 1H, Xanthene-*H*), 1.90 (s, 6H, *CMe*<sub>2</sub>).  $^{13}\text{C}\{^1\text{H}\}$  NMR (125.77 MHz,  $\text{CDCl}_3$ ):  $\delta$  (ppm) 171.4 (s), 158.3 (s), 150.9 (d,  $J_{\text{P-C}} = 5$  Hz), 146.5 (s), 145.3 (s), 133.4 (s), 133.3 (s), 133.2 (s), 132.58 (s), 132.56 (s), 132.2 (s), 131.5 (s), 131.4 (s), 131.29 (s), 131.25 (s), 131.0 (s), 130.9 (d,  $J_{\text{P-C}} = 5$  Hz), 129.5 (s), 129.4 (s), 128.3 (s), 127.8 (s), 125.1 (s), 125.0 (s), 123.8 (s), 120.2 (s), 118.9 (s), 115.8 (d,  $J_{\text{P-C}} = 60$  Hz), 34.7 (s), 33.4 (s).  $^{31}\text{P}\{^1\text{H}\}$  NMR (161.95 MHz,  $\text{CDCl}_3$ ):  $\delta$  (ppm) 23.3 (s).  $^{19}\text{F}$  NMR (376.42 MHz,  $\text{CDCl}_3$ ):  $\delta$  (ppm) -154.0 (s).  $^{11}\text{B}\{^1\text{H}\}$  NMR (128.40 MHz,  $\text{CDCl}_3$ ):  $\delta$  (ppm) -1.2 (s). **Elemental Analysis** calculated: C: 53.81, H: 3.39, found: C: 53.74, H: 3.49.

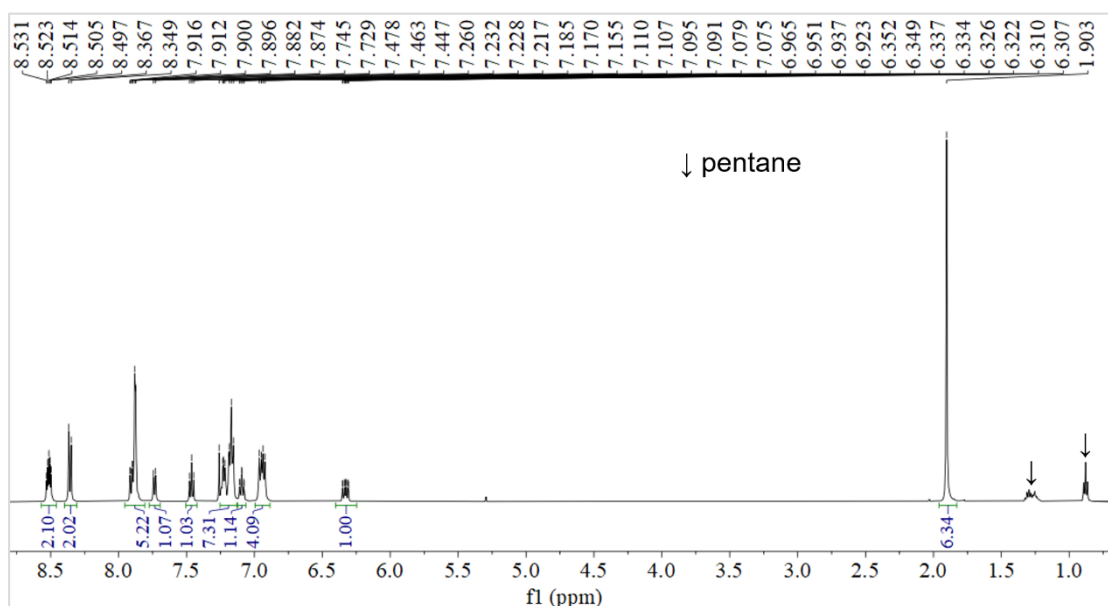


**Figure S12:**  $^1\text{H}$  NMR spectrum of  $[\mathbf{3}][\text{BF}_4]$  (500.13 MHz,  $\text{CDCl}_3$ ).

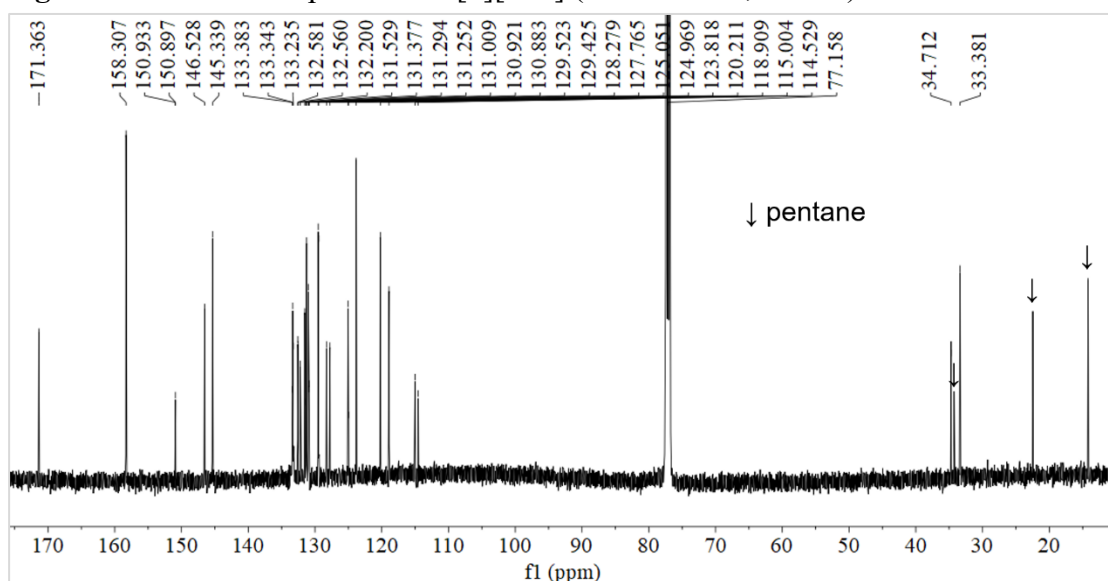


**Figure S13:**  $^{13}\text{C}\{^1\text{H}\}$  NMR spectrum of  $[\mathbf{3}][\text{BF}_4]$  (125.77 MHz,  $\text{CDCl}_3$ ).

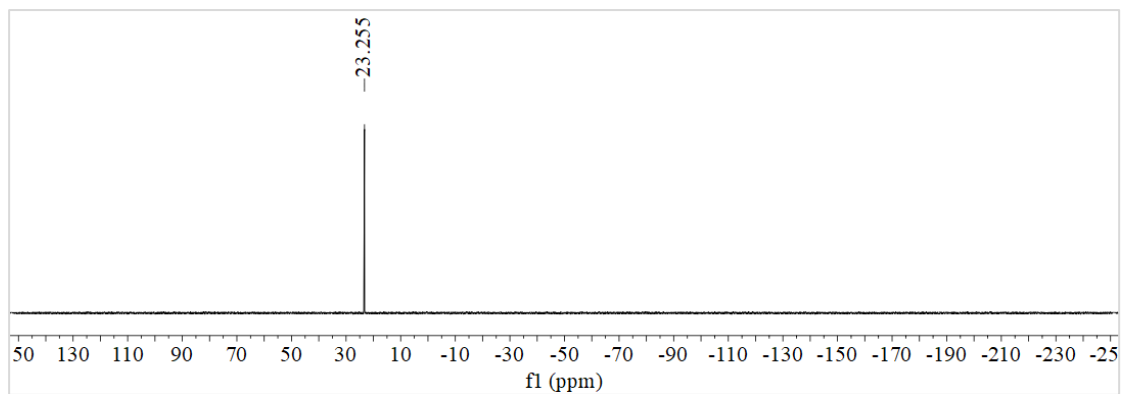


**Figure S14:**  $^{31}\text{P}\{^1\text{H}\}$  NMR spectrum of  $[\mathbf{3}][\text{BF}_4]$  (161.95 MHz,  $\text{CDCl}_3$ ).

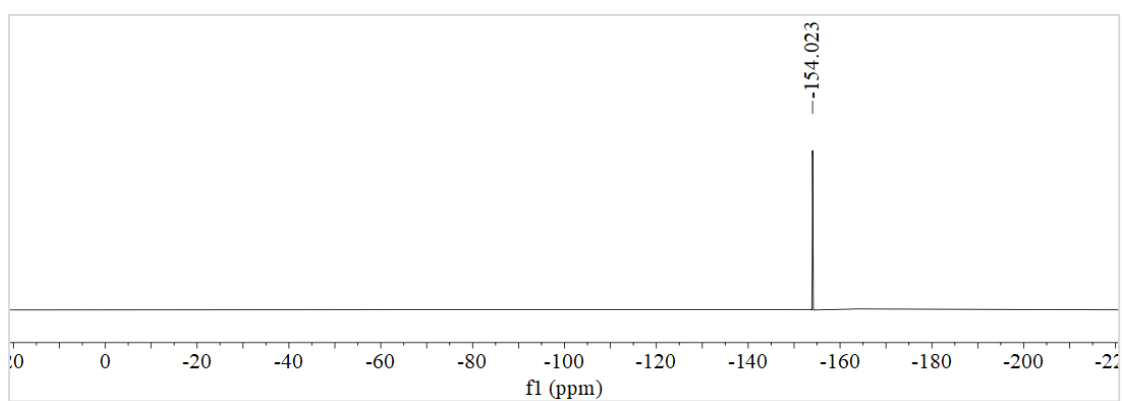


**Figure S15:**  $^{19}\text{F}$  NMR spectrum of  $[\mathbf{3}][\text{BF}_4]$  (376.42 MHz,  $\text{CDCl}_3$ ).

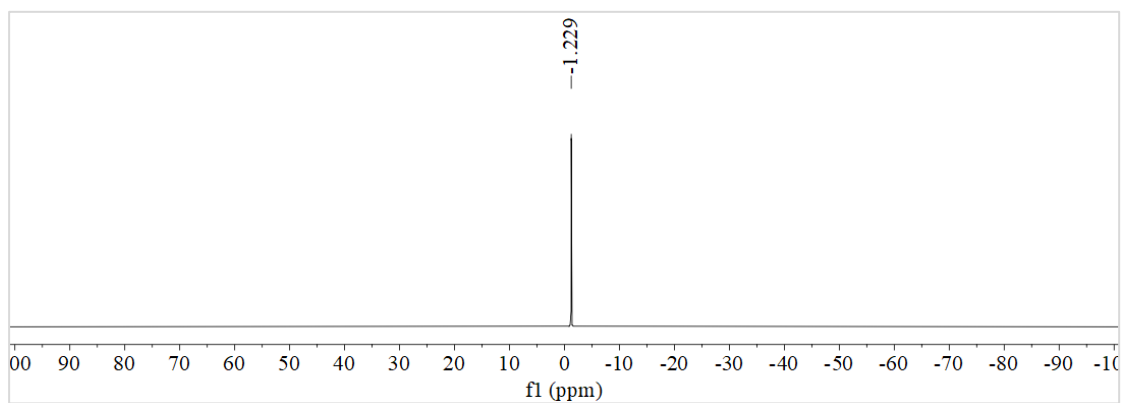
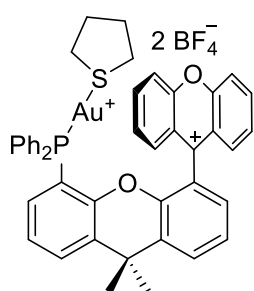


**Figure S16:**  $^{11}\text{B}\{^1\text{H}\}$  NMR spectrum of  $[\mathbf{3}][\text{BF}_4]$  (128.40 MHz,  $\text{CDCl}_3$ ).

### Synthesis of [4][BF<sub>4</sub>]<sub>2</sub>



[3][BF<sub>4</sub>] (26.8 mg, 0.03 mmol) and AgBF<sub>4</sub> (5.8 mg, 0.03 mmol) were mixed in dry CH<sub>2</sub>Cl<sub>2</sub> (1 mL). The resulting mixture was stirred at room temperature for 15 min. at which point tetrahydrothiophene (5.3 mg, 0.06 mmol) was added to the solution. The mixture was stirred at room temperature for 15 min. and filtered over a small plug of toilet paper placed in a pipette. The filtrate was combined with pentane (5 mL) under vigorous stirring.

The resulting precipitate was separated by decantation and dried under vacuum to give [4][BF<sub>4</sub>]<sub>2</sub> as a yellow solid (28.0 mg, 90% yield). Red crystals of [4][BF<sub>4</sub>]<sub>2</sub> were obtained from a 1,2-difluorobenzene solution upon diffusion of hexane. <sup>1</sup>H NMR (500.13 MHz, CD<sub>2</sub>Cl<sub>2</sub>): δ (ppm) 8.56 (m, 4H, Xanthylum-*H*), 7.99 (dd, <sup>3</sup>J<sub>H-H</sub> = 8 Hz, <sup>3</sup>J<sub>H-H</sub> = 2 Hz, 1H, Xanthene-*H*), 7.94 (m, 4H, Xanthylum-*H*), 7.85 (d, <sup>3</sup>J<sub>H-H</sub> = 8 Hz, 1H, Xanthene-*H*), 7.50 (t, <sup>3</sup>J<sub>H-H</sub> = 8 Hz, 1H, Xanthene-*H*), 7.31-7.14 (m, 1H, Xanthene-*H* and 6H, Ph-*H*), 7.03 (dd, <sup>3</sup>J<sub>H-H</sub> = 8 Hz, <sup>3</sup>J<sub>H-H</sub> = 2 Hz, 1H, Xanthene-*H*), 6.95 (m, 4H, Ph-*H*), 6.44 (ddd, <sup>3</sup>J<sub>H-P</sub> = 14 Hz, <sup>3</sup>J<sub>H-H</sub> = 8 Hz, <sup>4</sup>J<sub>H-H</sub> = 2 Hz, 1H, Xanthene-*H*), 3.43 (m, 4H, SCH<sub>2</sub>), 2.15 (m, 4H, SCH<sub>2</sub>CH<sub>2</sub>), 1.93 (s, 6H, CMe<sub>2</sub>). <sup>13</sup>C{<sup>1</sup>H} NMR (125.77 MHz, CD<sub>2</sub>Cl<sub>2</sub>): δ (ppm) 172.2 (s), 158.6 (s), 151.3 (d, J<sub>P-C</sub> = 5 Hz), 146.8 (s), 145.4 (s), 134.1 (d, J<sub>P-C</sub> = 6 Hz), 133.7 (s), 133.6 (s), 133.40 (s), 133.38 (s), 132.6 (d, J<sub>P-C</sub> = 2 Hz), 132.4 (s), 132.1 (s), 132.0 (s), 131.9 (s), 131.6 (d, J<sub>P-C</sub> = 5 Hz), 130.8 (s), 130.25 (s), 130.15 (s), 126.8 (s), 126.3 (s), 125.7 (d, J<sub>P-C</sub> = 11 Hz), 125.4 (s), 123.9 (s), 121.5 (s), 118.9 (s), 113.1 (d, J<sub>P-C</sub> = 60 Hz), 39.8 (br), 35.1 (s), 33.2 (br), 31.5 (s). <sup>31</sup>P{<sup>1</sup>H} NMR (161.95 MHz, CD<sub>2</sub>Cl<sub>2</sub>): δ (ppm) 26.4 (s). <sup>19</sup>F NMR (376.42 MHz, CD<sub>2</sub>Cl<sub>2</sub>): δ (ppm) -152.4 (m). <sup>11</sup>B{<sup>1</sup>H} NMR (128.40 MHz, CD<sub>2</sub>Cl<sub>2</sub>): δ (ppm) -1.1 (s). **Elemental Analysis** calculated: C: 51.19, H: 3.71, found: C: 51.25, H: 3.71.

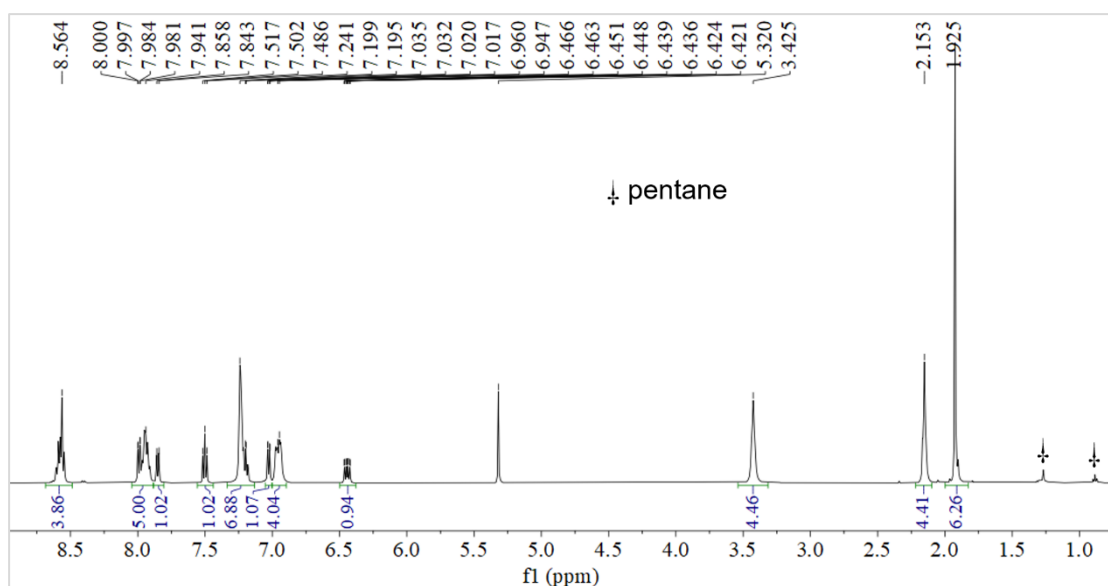


**Figure S17:**  $^1\text{H}$  NMR spectrum of  $[\mathbf{4}][\text{BF}_4]_2$  (500.13 MHz,  $\text{CD}_2\text{Cl}_2$ ).

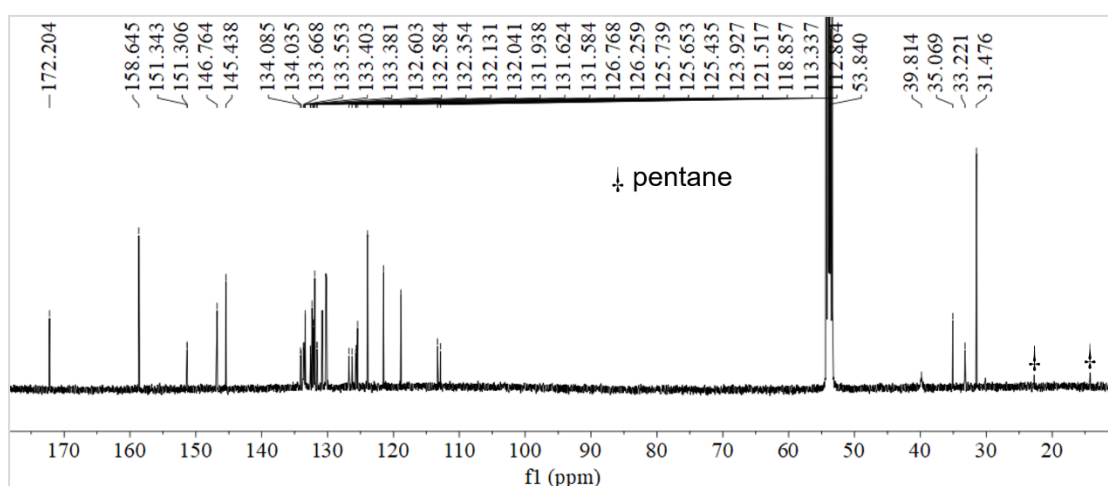


**Figure S18:**  $^{13}\text{C}\{^1\text{H}\}$  NMR spectrum of  $[\mathbf{4}][\text{BF}_4]_2$  (125.77 MHz,  $\text{CD}_2\text{Cl}_2$ ).

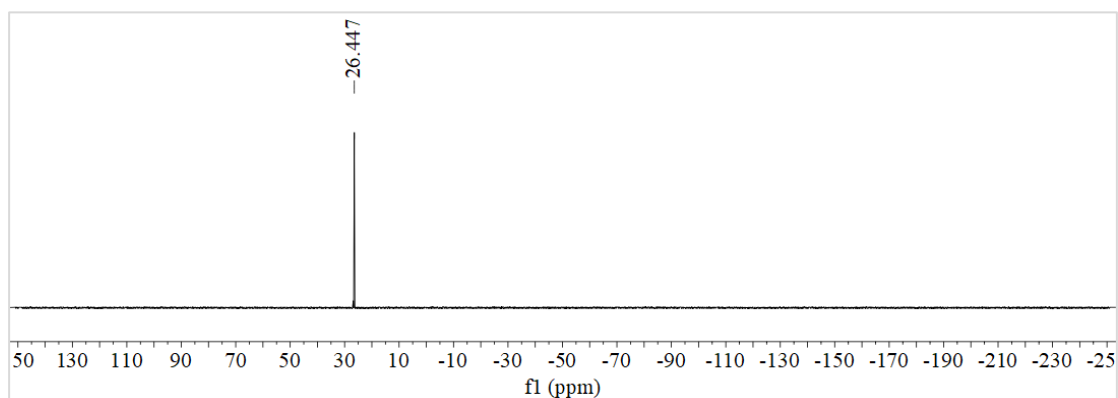


**Figure S19:**  $^{31}\text{P}\{^1\text{H}\}$  NMR spectrum of  $[\mathbf{4}][\text{BF}_4]_2$  (161.95 MHz,  $\text{CD}_2\text{Cl}_2$ ).

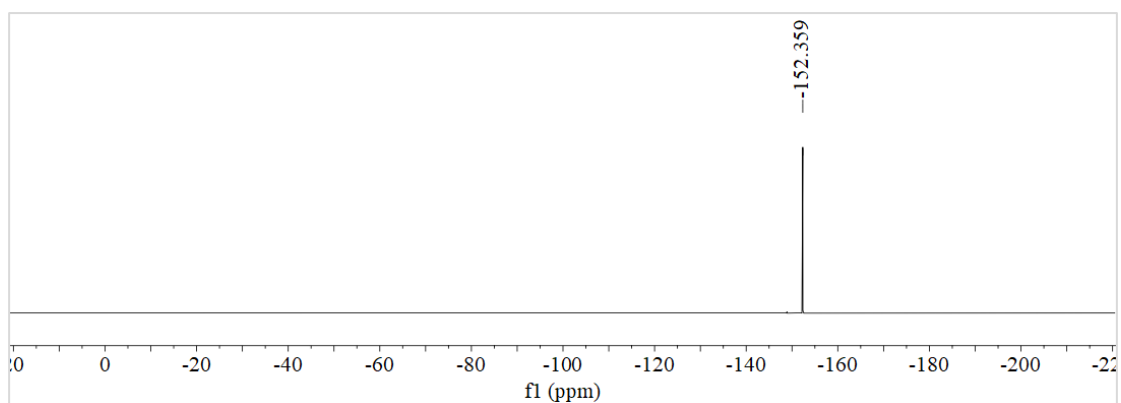


**Figure S20:**  $^{19}\text{F}$  NMR spectrum of  $[\mathbf{4}][\text{BF}_4]_2$  (376.42 MHz,  $\text{CD}_2\text{Cl}_2$ ).

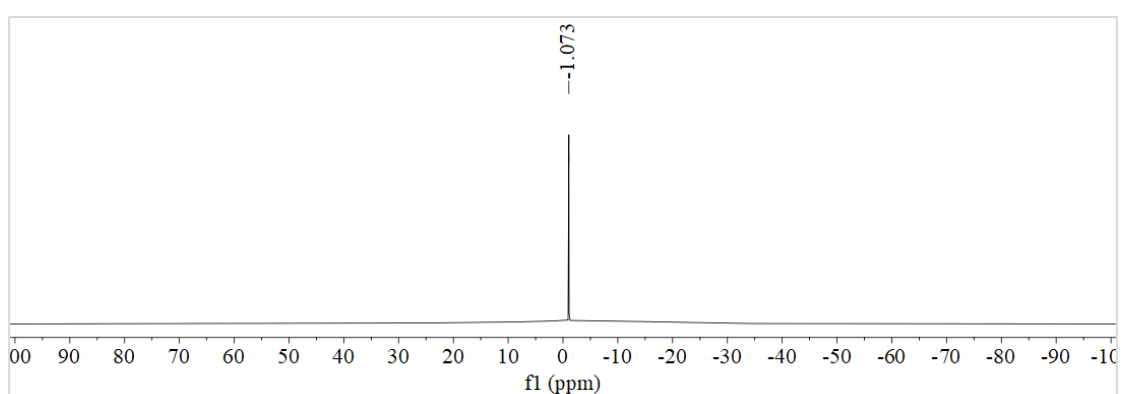


**Figure S21:**  $^{11}\text{B}\{^1\text{H}\}$  NMR spectrum of  $[\mathbf{4}][\text{BF}_4]_2$  (128.40 MHz,  $\text{CD}_2\text{Cl}_2$ ).

Generation of  $[\mathbf{4}][\text{BF}_4]_2$  via addition of tht to **Int**

$[\mathbf{3}][\text{BF}_4]$  (8.9 mg, 0.01 mmol) and  $\text{AgBF}_4$  (1.9 mg, 0.01 mmol) were mixed in  $\text{CD}_2\text{Cl}_2$  (0.6 mL). The resulting mixture was stirred at room temperature for 15 min., then filtered, and transferred into an NMR tube for NMR spectroscopy analysis. After recording the first spectra which confirmed the formation of **Int**, tht (0.9 mg, 0.01 mmol) was added into the solution, and the mixture was again subjected to NMR spectroscopy analysis. This experiments showed conversion of **Int** into  $[\mathbf{4}][\text{BF}_4]_2$ .

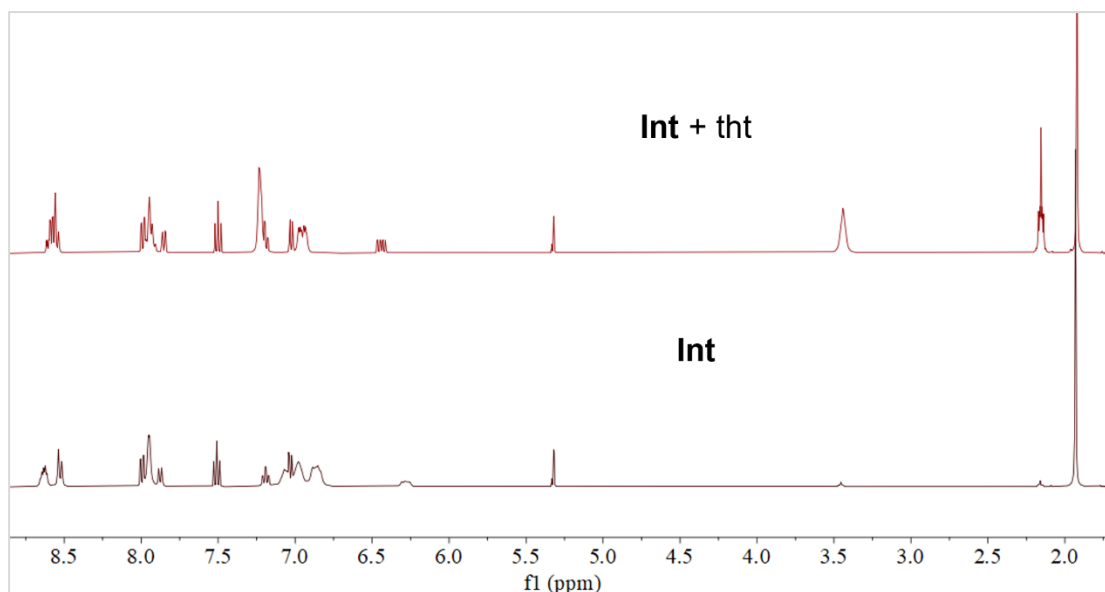


**Figure S22:**  $^1\text{H}$  NMR spectra of **Int** generated *in situ* before and after its reaction with tht (400.09 MHz,  $\text{CD}_2\text{Cl}_2$ ).

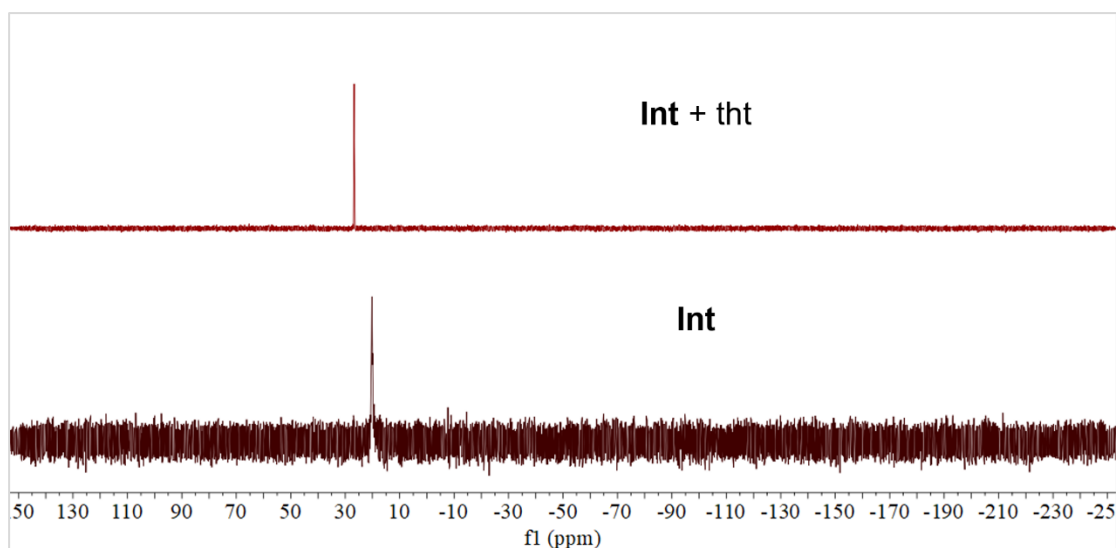
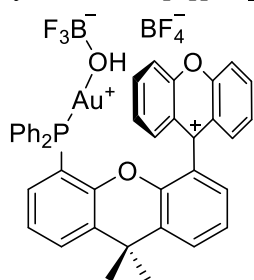


**Figure S23:** Comparative *in situ*  $^{31}\text{P}\{^1\text{H}\}$  NMR spectra of **Int** and reaction with tht (161.95 MHz,  $\text{CD}_2\text{Cl}_2$ ).

#### Synthesis of **[5][BF<sub>4</sub>]**



**[3][BF<sub>4</sub>]** (17.9 mg, 0.02 mmol) and  $\text{AgBF}_4$  (3.9 mg, 0.02 mmol) were combined in dry  $\text{CH}_2\text{Cl}_2$  (1 mL) to afford a heterogeneous mixture. After stirring at room temperature for 30 min, the reaction mixture was treated with water (0.8  $\mu\text{L}$ , 0.044 mmol) and stirring was continued for 4 h at room temperature. The reaction mixture was then filtered and the filtrate was combined with

pentane (5 mL) under vigorous stirring. The resulting precipitate was separated by decantation and dried under vacuum to afford [5][BF<sub>4</sub>] as a crude yellow solid. Yellow crystals of [5][BF<sub>4</sub>]·0.53(C<sub>6</sub>H<sub>4</sub>F<sub>2</sub>)·0.47(hexane) were obtained by diffusion of hexane into a 1,2-difluorobenzene solution of the crude product at room temperature and dried under vacuum to give [5][BF<sub>4</sub>] as a yellow solid (12.3 mg, 65% yield). <sup>1</sup>H NMR (400.09 MHz, CD<sub>2</sub>Cl<sub>2</sub>): δ (ppm) 8.61 (ddd, <sup>3</sup>J<sub>H-H</sub> = 9 Hz, <sup>3</sup>J<sub>H-H</sub> = 6 Hz, <sup>4</sup>J<sub>H-H</sub> = 3 Hz, 2H, Xanthylium-*H*), 8.44 (d, <sup>3</sup>J<sub>H-H</sub> = 9 Hz, 2H, Xanthylium-*H*), 7.98 (m, 4H, Xanthylium-*H* and 1H, Xanthene-*H*), 7.80 (d, <sup>3</sup>J<sub>H-H</sub> = 8 Hz, 1H, Xanthene-*H*), 7.48 (t, <sup>3</sup>J<sub>H-H</sub> = 8 Hz, 1H, Xanthene-*H*), 7.27-6.86 (m, 4H, Xanthene-*H* and 10H, Ph-*H*), 6.38 (ddd, <sup>3</sup>J<sub>H-P</sub> = 14 Hz, <sup>3</sup>J<sub>H-H</sub> = 8 Hz, <sup>4</sup>J<sub>H-H</sub> = 2 Hz, 1H, Xanthene-*H*), 4.20 (q, <sup>3</sup>J<sub>F-H</sub> = 4.5 Hz, 1H, BF<sub>3</sub>OH), 1.91 (s, 6H, CMe<sub>2</sub>). <sup>13</sup>C{<sup>1</sup>H} NMR (125.77 MHz, CD<sub>2</sub>Cl<sub>2</sub>): δ (ppm) 172.0 (s), 158.4 (s), 151.3 (d, *J*<sub>P-C</sub> = 4 Hz), 146.8 (s), 146.0 (s), 133.7 (br, 2C), 133.6 (s), 133.0 (br, 2C), 132.4 (s), 132.2 (s), 131.9 (s), 131.8 (s), 131.4 (d, *J*<sub>P-C</sub> = 5 Hz), 131.1 (s), 129.7 (s), 129.6 (s), 127.5 (s), 127.0 (s), 125.5 (s), 125.4 (s), 125.2 (s), 123.8 (s), 120.8 (s), 118.9 (s), 113.6 (d, *J*<sub>P-C</sub> = 70 Hz), 35.1 (s), 33.2 (s). <sup>31</sup>P{<sup>1</sup>H} NMR (161.95 MHz, CD<sub>2</sub>Cl<sub>2</sub>): δ (ppm) 17.2 (s). <sup>19</sup>F NMR (376.42 MHz, CD<sub>2</sub>Cl<sub>2</sub>): δ (ppm) -146.7 (m, <sup>19</sup>F-<sup>10</sup>B coupling) and -146.8 (dq, <sup>3</sup>J<sub>F-H</sub> = 4.5 Hz, <sup>1</sup>J<sub>F-B</sub> = 6.7 Hz, <sup>19</sup>F-<sup>11</sup>B coupling) (BF<sub>3</sub>OH), -151.8 (m, BF<sub>4</sub>). <sup>11</sup>B{<sup>1</sup>H} NMR (128.40 MHz, CD<sub>2</sub>Cl<sub>2</sub>): δ (ppm) -0.3 (q, <sup>1</sup>J<sub>F-B</sub> = 6.7 Hz, BF<sub>3</sub>OH), -1.1 (s, BF<sub>4</sub>). **Elemental Analysis** calculated: C: 50.99, H: 3.32, found: C: 50.73, H: 3.40. IR (cm<sup>-1</sup>) ν(O-H) 3645 (br).

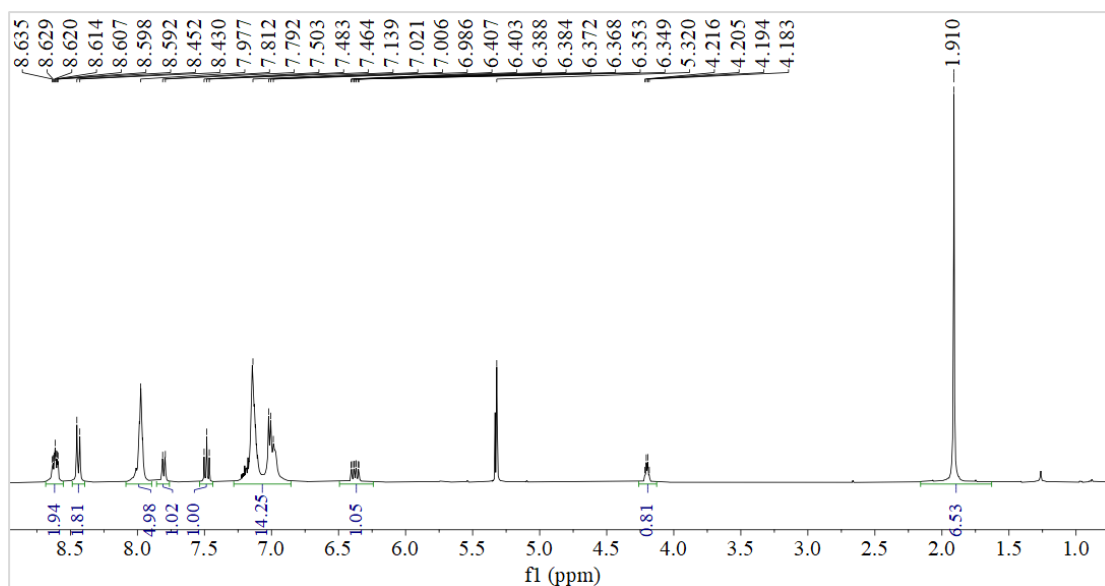


**Figure S24:** <sup>1</sup>H NMR spectrum of [5][BF<sub>4</sub>] (400.09 MHz, CD<sub>2</sub>Cl<sub>2</sub>).

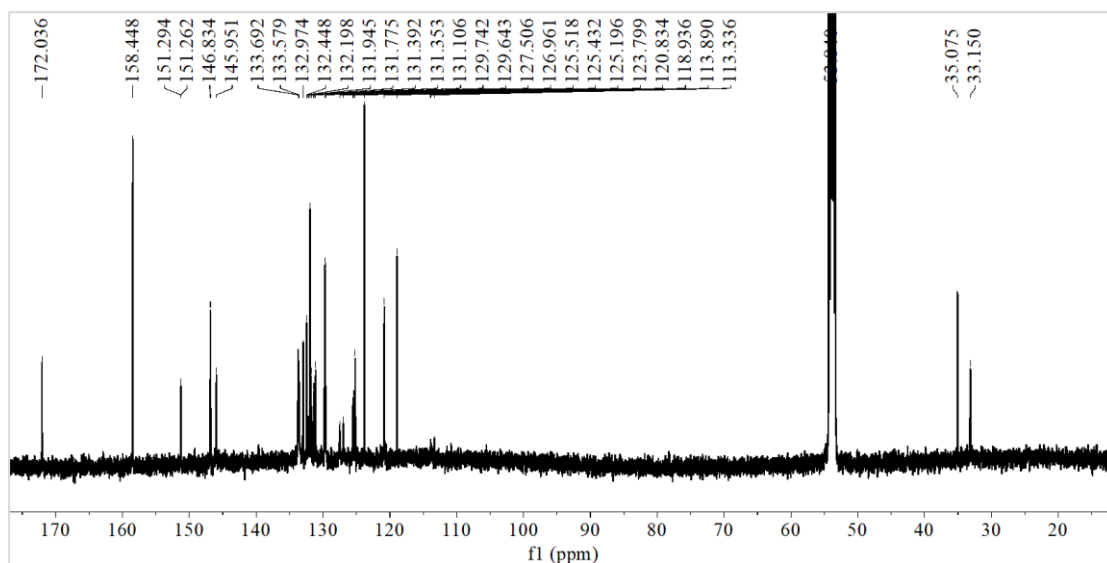


**Figure S25:**  $^{13}\text{C}\{^1\text{H}\}$  NMR spectrum of  $[\mathbf{5}][\text{BF}_4]$  (125.77 MHz,  $\text{CD}_2\text{Cl}_2$ ).

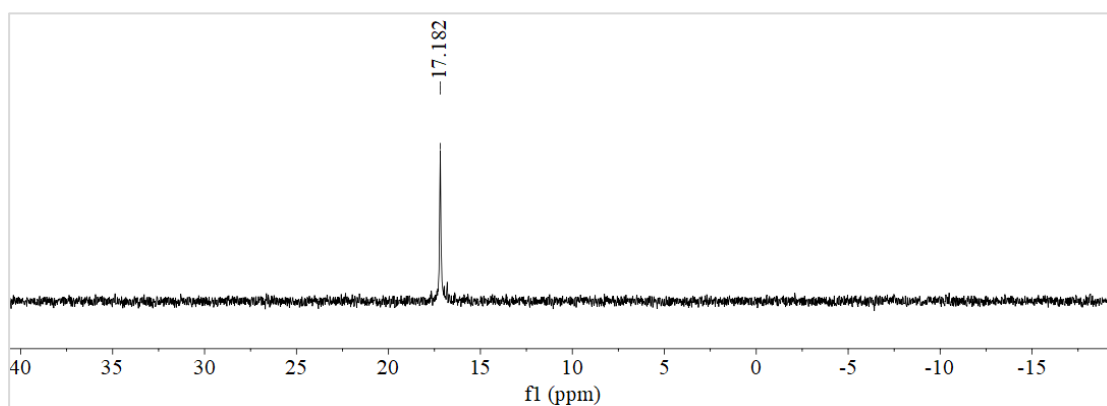


**Figure S26:**  $^{31}\text{P}\{^1\text{H}\}$  NMR spectrum of  $[\mathbf{5}][\text{BF}_4]$  (161.95 MHz,  $\text{CD}_2\text{Cl}_2$ ).

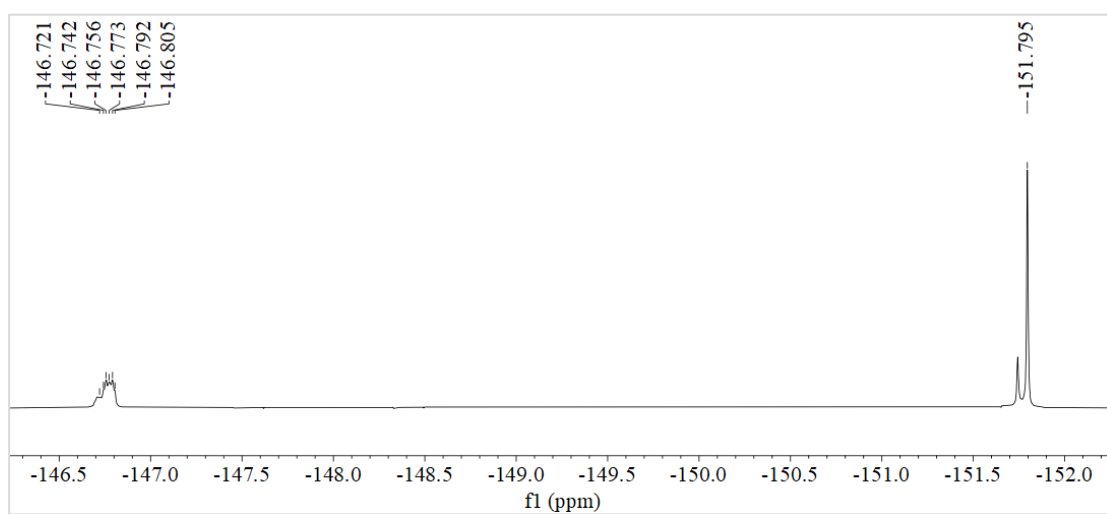


**Figure S27:**  $^{19}\text{F}$  NMR spectrum of  $[\mathbf{5}][\text{BF}_4]$  (376.42 MHz,  $\text{CD}_2\text{Cl}_2$ ).

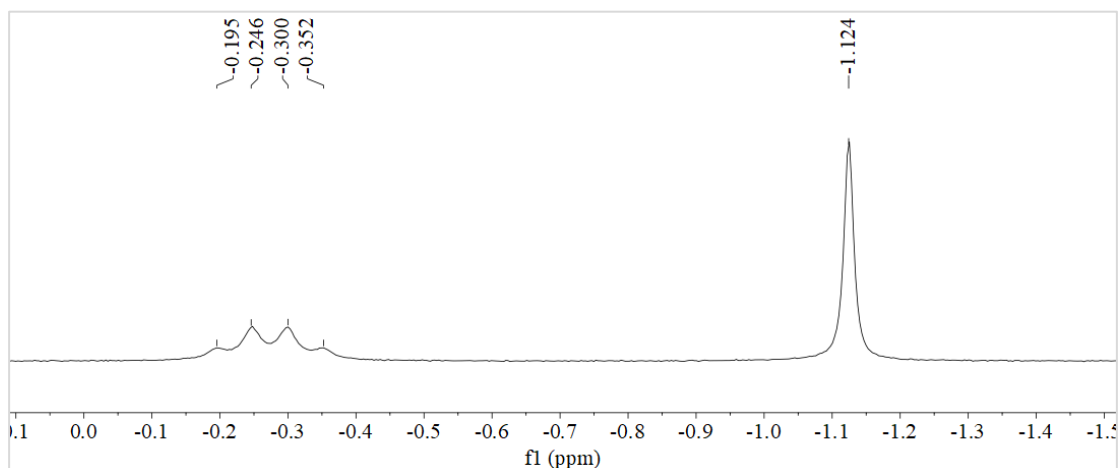


**Figure S28:**  $^{11}\text{B}\{^1\text{H}\}$  NMR spectrum of  $[\mathbf{5}][\text{BF}_4]$  (128.40 MHz,  $\text{CD}_2\text{Cl}_2$ ).

**Generation of  $[\mathbf{5}][\text{BF}_4]_2$  via addition of water to **Int****

$[\mathbf{3}][\text{BF}_4]$  (8.9 mg, 0.01 mmol) and  $\text{AgBF}_4$  (1.9 mg, 0.01 mmol) were mixed in  $\text{CD}_2\text{Cl}_2$  (0.6 mL). The resulting mixture was stirred at room temperature for 15 min., then filtered, and transferred into an NMR tube for NMR spectroscopy analysis. After recording the first spectra which confirmed the formation of **Int**, water (0.2 mg, 0.011 mmol) was added into the solution, and the mixture was again subjected to NMR spectroscopy analysis. This experiments showed conversion of **Int** into  $[\mathbf{5}][\text{BF}_4]_2$ .

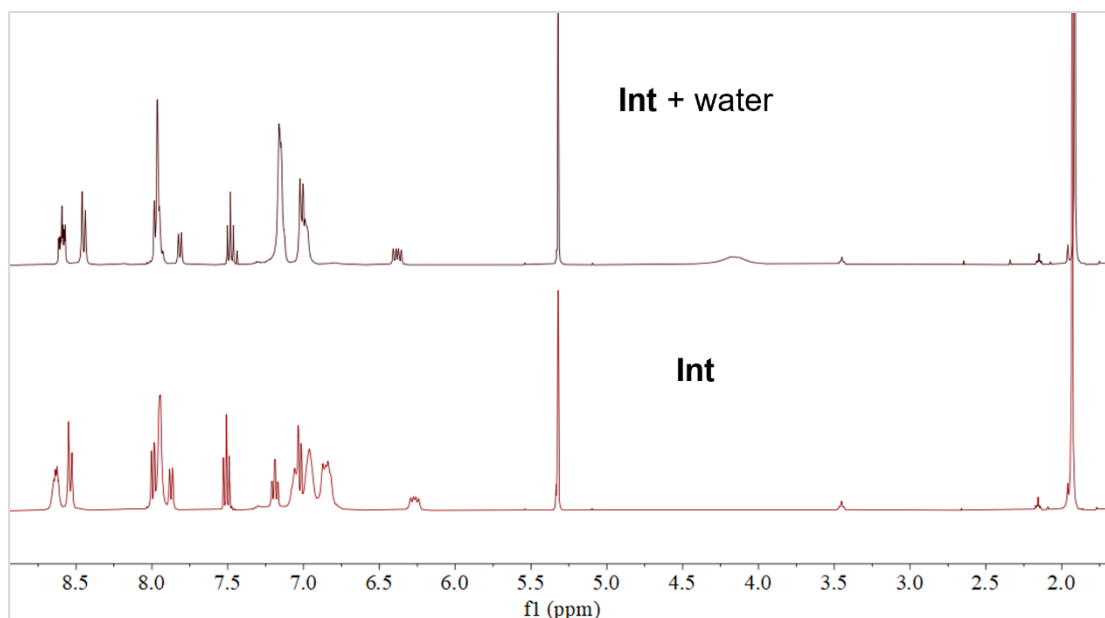


**Figure S29:**  $^1\text{H}$  NMR spectra of **Int** generated *in situ* before and after its reaction with water (400.09 MHz,  $\text{CD}_2\text{Cl}_2$ ).

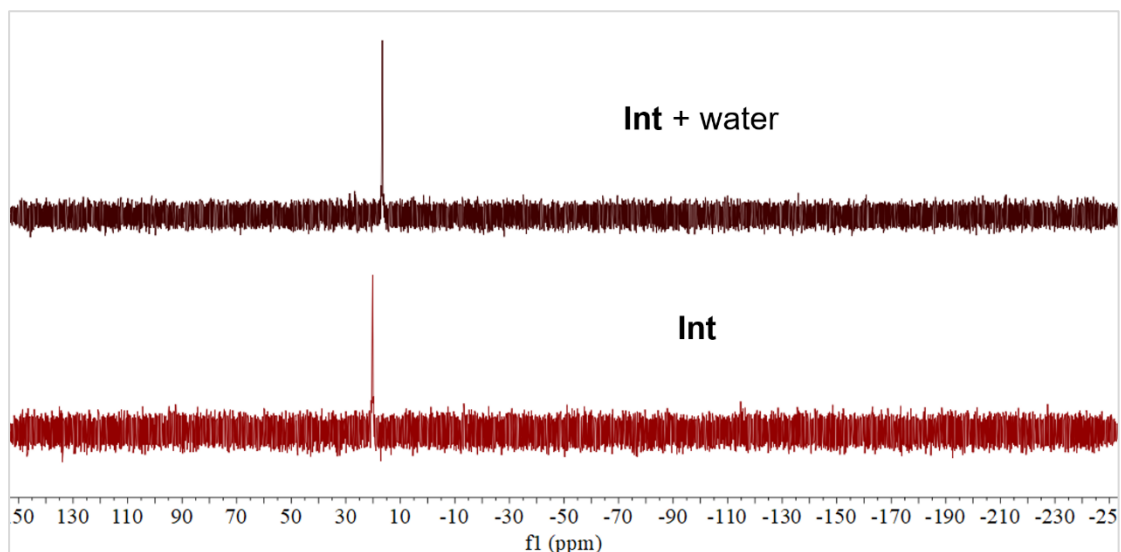


**Figure S30:** Comparative *in situ*  $^{31}\text{P}\{^1\text{H}\}$  NMR spectra of **Int** and reaction with water (161.95 MHz,  $\text{CD}_2\text{Cl}_2$ ).

Reaction of  $\text{Ph}_3\text{PAuCl}$  with  $\text{AgBF}_4$  and water.

$\text{Ph}_3\text{PAuCl}$  (9.9 mg, 0.02 mmol) and  $\text{AgBF}_4$  (3.9 mg, 0.02 mmol) were mixed in dry  $\text{CD}_2\text{Cl}_2$  (0.6 mL). The resulting mixture was stirred at room temperature for 15 min., then filtered. Water (0.4  $\mu\text{L}$ , 0.4 mg, 0.022 mmol) was added to the solution. The solution was transferred into an NMR tube for NMR spectroscopy analysis. The  $^1\text{H}$ ,  $^{13}\text{C}$ , and  $^{31}\text{P}$  NMR data of the solution is consistent with that reported for  $[\text{Ph}_3\text{PAu}(\text{OH}_2)][\text{OTf}]$ ,<sup>2</sup> indicating the generation of  $[\text{Ph}_3\text{PAu}(\text{OH}_2)][\text{BF}_4]$ . The  $^{19}\text{F}$ , and  $^{11}\text{B}$  NMR spectra of the solution (**Figure S34** and **Figure S35**) displays resonances indicating the trace presence of  $[\text{BF}_3\text{OH}]^-$ .  $^1\text{H}$  NMR (400.09 MHz,  $\text{CD}_2\text{Cl}_2$ ):  $\delta$  (ppm) 7.59 (m, 3H, Ph-H), 7.47 (m, 12H, Ph-H), 3.54 (br, 2H,  $\text{H}_2\text{O}$ ).  $^{13}\text{C}\{^1\text{H}\}$  NMR (100.61 MHz,  $\text{CD}_2\text{Cl}_2$ ):  $\delta$  (ppm) 134.4 (d,  $J_{\text{P-C}} = 14$  Hz), 133.2 (d,  $J_{\text{P-C}} = 3$  Hz), 130.0 (d,  $J_{\text{P-C}} = 12$  Hz), 127.2 (d,  $J_{\text{P-C}} = 67$  Hz).  $^{31}\text{P}\{^1\text{H}\}$  NMR (161.95 MHz,  $\text{CD}_2\text{Cl}_2$ ):  $\delta$  (ppm) 28.6 (s, 1P,  $[\text{Ph}_3\text{PAu}(\text{OH}_2)]^+$ ).  $^{19}\text{F}$  NMR (377 MHz,  $\text{CD}_2\text{Cl}_2$ ): -151.8 (m,  $\text{BF}_4$ ).  $^{11}\text{B}\{^1\text{H}\}$  NMR (128 MHz,  $\text{CD}_2\text{Cl}_2$ ):  $\delta$  (ppm) -1.1 (s,  $\text{BF}_4$ ).

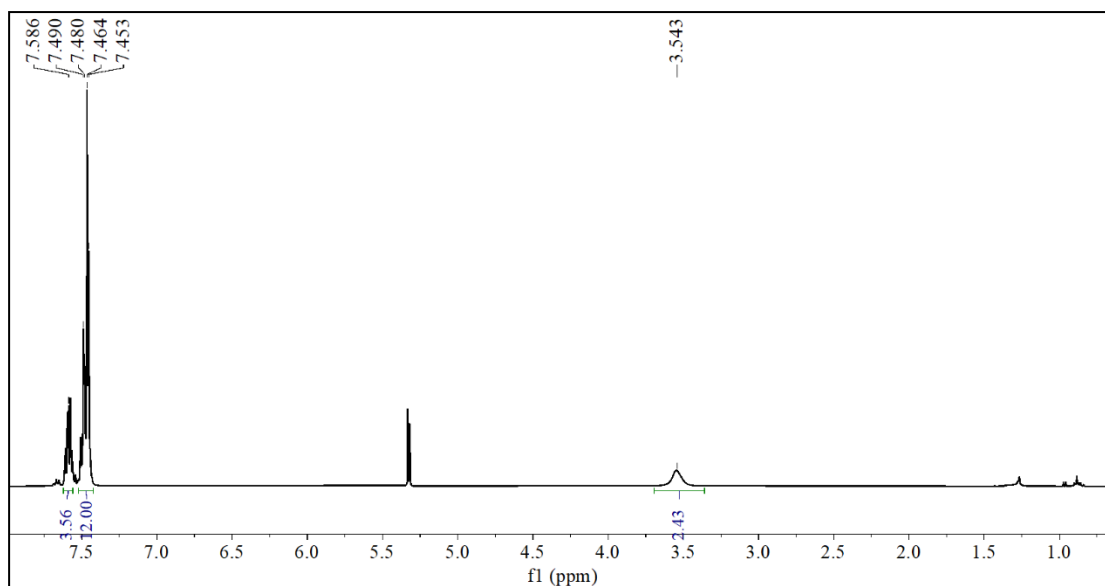


**Figure S31:**  $^1\text{H}$  NMR spectrum of  $[\text{Ph}_3\text{PAu}(\text{OH}_2)][\text{BF}_4]$  (400 MHz,  $\text{CD}_2\text{Cl}_2$ ).

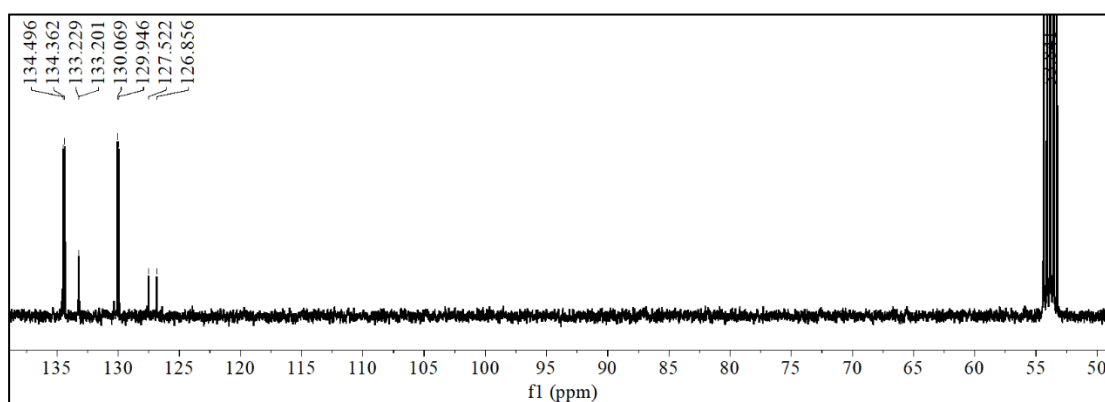


**Figure S32:**  $^{13}\text{C}\{^1\text{H}\}$  NMR spectrum of  $[\text{Ph}_3\text{PAu}(\text{OH}_2)][\text{BF}_4]$  (126 MHz,  $\text{CD}_2\text{Cl}_2$ ).

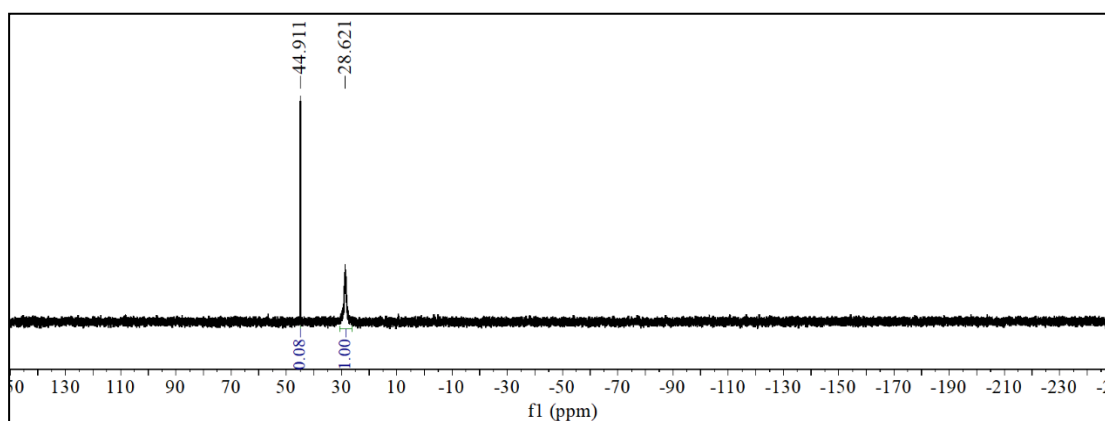


**Figure S33:**  $^{31}\text{P}\{^1\text{H}\}$  NMR spectrum of  $[\text{Ph}_3\text{PAu}(\text{OH}_2)][\text{BF}_4]$  (162 MHz,  $\text{CD}_2\text{Cl}_2$ ). The main resonance corresponds to  $[\text{Ph}_3\text{PAu}(\text{OH}_2)]^+$ . The peak at -44.01 corresponds to traces of  $[(\text{Ph}_3\text{P})_2\text{Au}]^+$ .

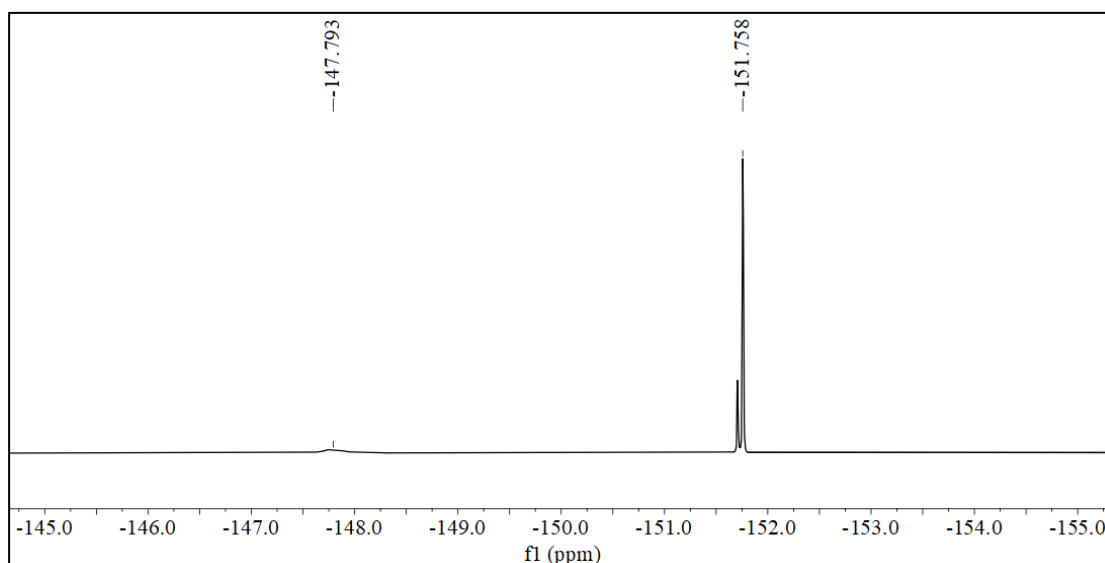


**Figure S34:**  $^{19}\text{F}$  NMR spectrum of  $[\text{Ph}_3\text{PAu}(\text{OH}_2)][\text{BF}_4]$  (377 MHz,  $\text{CD}_2\text{Cl}_2$ ). The main resonance corresponds to  $[\text{BF}_4]^-$ . The resonance at -147.79 ppm corresponds to traces of  $[\text{BF}_3\text{OH}]^-$ .

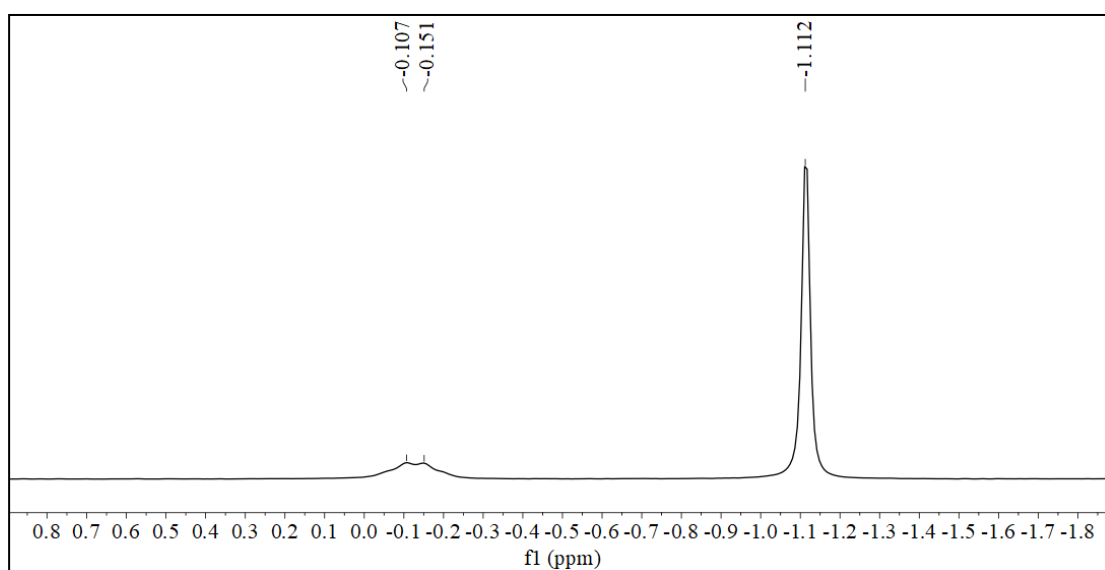
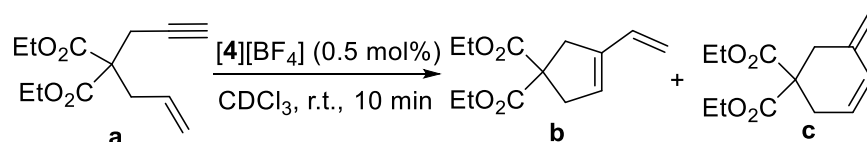


**Figure S35:**  $^{11}\text{B}\{^1\text{H}\}$  NMR spectrum of  $[\text{Ph}_3\text{PAu}(\text{OH}_2)][\text{BF}_4]$  (128 MHz,  $\text{CD}_2\text{Cl}_2$ ). The main resonance corresponds to  $[\text{BF}_4]^-$ . The resonance at -0.13 ppm corresponds to traces of  $[\text{BF}_3\text{OH}]^-$ .

## 2.2 Catalysis studies

### 2.2.1 Evaluation of [5]BF<sub>4</sub> as a catalyst

Reaction 1: Cycloisomerization reaction of **a**:



A CH<sub>2</sub>Cl<sub>2</sub> solution of [5][BF<sub>4</sub>] (0.02 M, 25  $\mu$ L, 0.0005 mmol) was added to a solution of enyne **a** (0.1 mmol, 23.8 mg) in CDCl<sub>3</sub> (0.6 mL) which was used as commercially provided. The mixture was transferred into an NMR tube and the reaction was monitored *in situ* by <sup>1</sup>H NMR spectroscopy at room temperature. The <sup>1</sup>H NMR spectra collected are consistent with the formation of **b** and **c** as supported by literature precedents.<sup>3</sup> **b** : **c** = 22 : 78. **b**: <sup>1</sup>H NMR (400.09 MHz, CDCl<sub>3</sub>):  $\delta$  (ppm) 6.47 (dd, <sup>3</sup>J<sub>H-H</sub> = 17 Hz, <sup>3</sup>J<sub>H-H</sub> = 11 Hz, 1H, CH=CH<sub>2</sub>), 5.57 (m, 1H, CH<sub>2</sub>-CH), 5.09 (d, <sup>3</sup>J<sub>H-H</sub> = 17 Hz, 1H, CH=CH<sub>2</sub>), 5.08 (d, <sup>3</sup>J<sub>H-H</sub> = 10 Hz, 1H, CH=CH<sub>2</sub>), 4.20 (m, 4H, OCH<sub>2</sub>CH<sub>3</sub>), 3.11 (m, 2H, CH<sub>2</sub>CCH<sub>2</sub>), 3.09 (m, 2H, CH<sub>2</sub>CCH<sub>2</sub>), 1.25 (t, <sup>3</sup>J<sub>H-H</sub> = 7 Hz, 6H, OCH<sub>2</sub>CH<sub>3</sub>). **c**: <sup>1</sup>H NMR (400.09 MHz, CDCl<sub>3</sub>):  $\delta$  (ppm) 6.14 (dt, <sup>3</sup>J<sub>H-H</sub> = 10 Hz, <sup>4</sup>J<sub>H-H</sub> = 2 Hz, 1H, CH=CHCH<sub>2</sub>), 5.77 (m, 1H, CH=CHCH<sub>2</sub>), 4.91 (m, 1H, C=CH<sub>2</sub>), 4.89 (m, 1H, C=CH<sub>2</sub>), 4.16 (m, 4H, OCH<sub>2</sub>CH<sub>3</sub>), 2.85 (t, <sup>4</sup>J<sub>H-H</sub> = 2 Hz, 2H, CH<sub>2</sub>C=CH<sub>2</sub>), 2.67 (m, 2H, CH<sub>2</sub>CH=CH), 1.22 (t, <sup>3</sup>J<sub>H-H</sub> = 7 Hz, 6H, OCH<sub>2</sub>CH<sub>3</sub>).

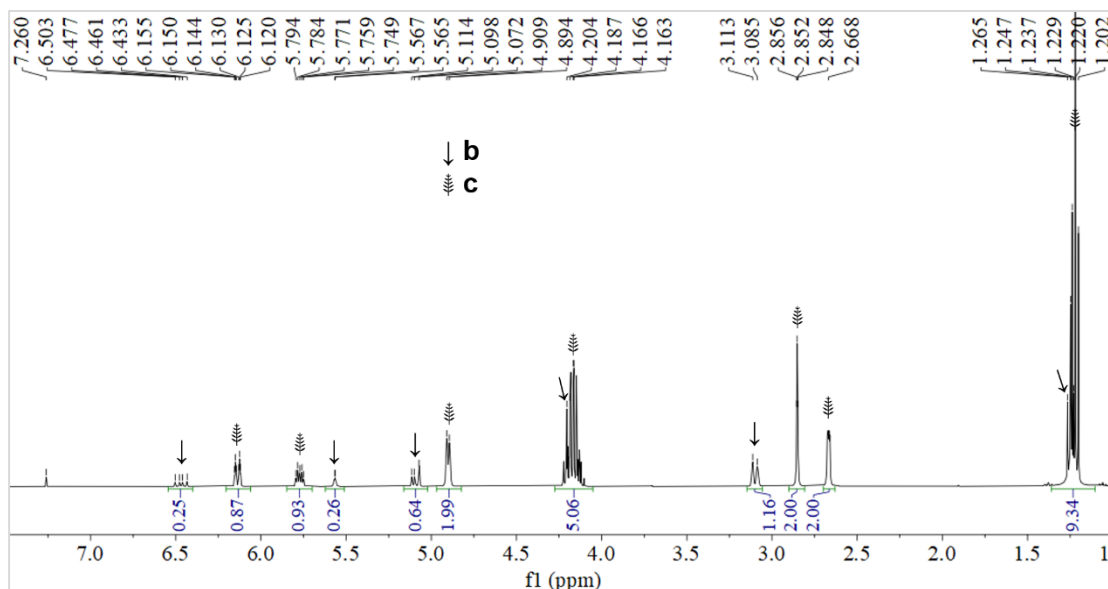
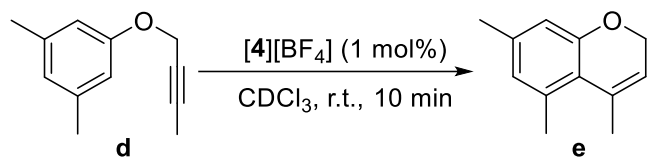


**Figure S36:** *In situ* <sup>1</sup>H NMR spectrum of the cycloisomerization reaction of **a** catalyzed by [5][BF<sub>4</sub>] at room temperature (400.09 MHz, CDCl<sub>3</sub>). This spectrum was obtained 10 min. after mixing.

Reaction 2: Cyclization reaction of **d**.



A  $\text{CH}_2\text{Cl}_2$  solution of **[5][BF<sub>4</sub>]** (0.02 M, 50  $\mu\text{L}$ , 0.001 mmol) was added to a solution of **d** (0.1 mmol, 17.4 mg) in  $\text{CDCl}_3$  (0.6 mL) which was used as commercially provided. The mixture was transferred into an NMR tube and the reaction was monitored *in situ* by  $^1\text{H}$  NMR spectroscopy at room temperature. The  $^1\text{H}$  NMR spectra collected are consistent with the formation of **e** as supported by literature precedents.<sup>3</sup>  $^1\text{H}$  NMR (400.09 MHz,  $\text{CDCl}_3$ ):  $\delta$  (ppm) 6.59 (s, 1H, Ar-*H*), 6.58 (s, 1H, Ar-*H*), 5.65 (tq,  $^3J_{\text{H-H}} = 5$  Hz,  $^4J_{\text{H-H}} = 2$  Hz, 1H,  $\text{OCH}_2\text{CH}$ ), 4.42 (dq,  $^3J_{\text{H-H}} = 5$  Hz,  $^5J_{\text{H-H}} = 2$  Hz, 2H,  $\text{OCH}_2\text{CH}$ ), 2.44 (s, 3H, Ar $\text{CH}_3$ ), 2.25 (s, 3H, Ar $\text{CH}_3$ ), 2.18 (q,  $^4J_{\text{H-H}} = ^5J_{\text{H-H}} = 2$  Hz, 3H,  $\text{OCH}_2\text{CH}=\text{CCH}_3$ ).

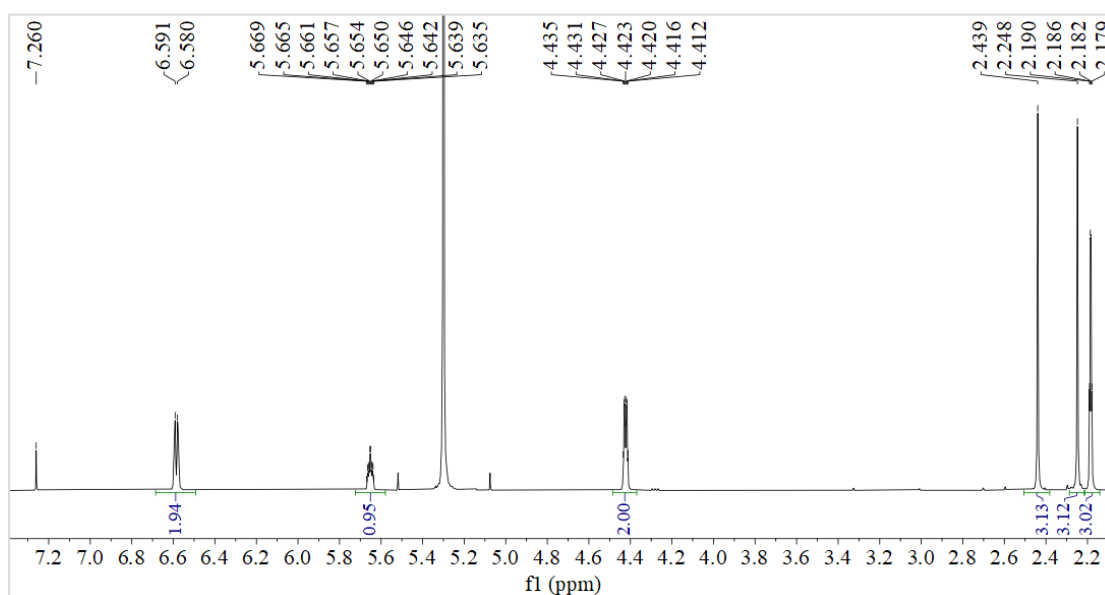
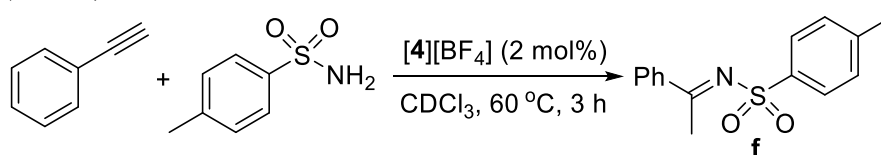
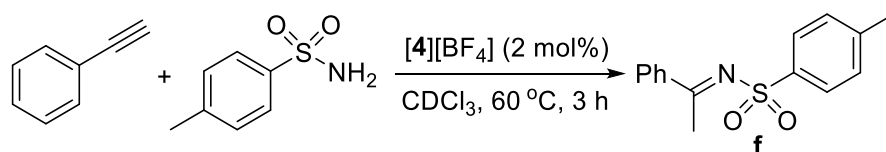


**Figure S37:** *In situ*  $^1\text{H}$  NMR spectrum of the cyclization reaction of **d** catalyzed by **[5][BF<sub>4</sub>]** at room temperature (400.09 MHz,  $\text{CDCl}_3$ ). This spectrum was obtained 10 min. after mixing.

Reaction 3: Hydroamination reaction of phenylacetylene with *p*-toluenesulfonamide ( $\text{TsNH}_2$ ).



### Experiment 1:



[5][BF<sub>4</sub>] (0.002 mmol, 1.9 mg), TsNH<sub>2</sub> (17.1 mg, 0.1 mmol) and phenylacetylene (10.2 mg, 0.1 mmol) were mixed in CH<sub>2</sub>Cl<sub>2</sub> (0.3 mL) and CDCl<sub>3</sub> (0.3 mL). The mixture was transferred into an NMR tube which was capped and placed into an oil bath heated to 60 °C. After 2 h, the solution was analyzed by <sup>1</sup>H NMR spectroscopy, which showed 85% of starting materials were converted to **f**.<sup>4</sup>

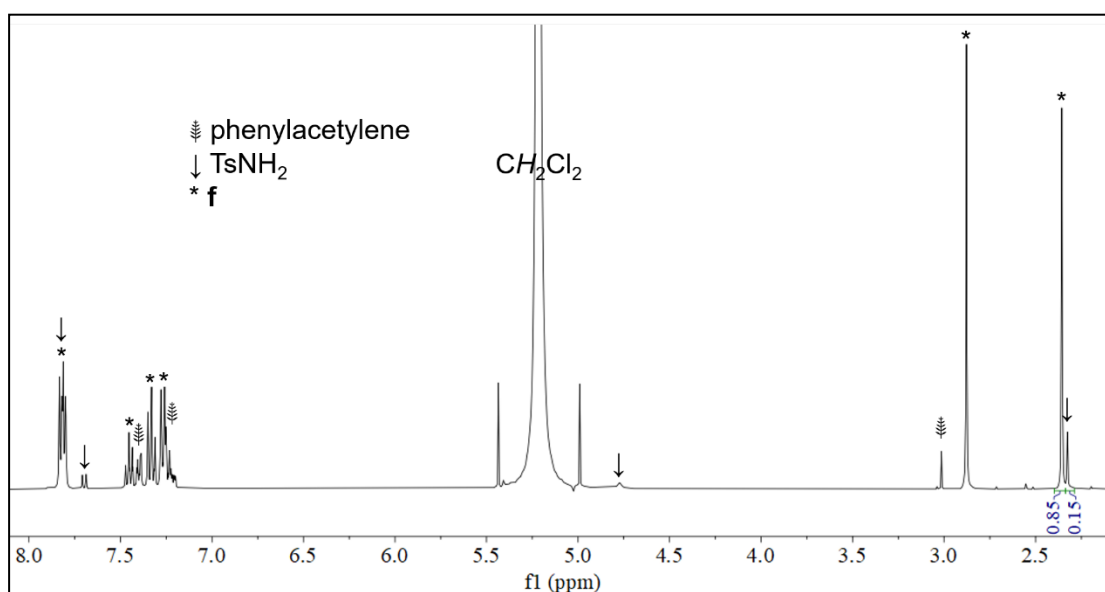


**Figure S38.** *In situ* <sup>1</sup>H NMR spectrum of the hydroamination reaction of phenylacetylene catalyzed by [5][BF<sub>4</sub>] at 60 °C for 2 h (400.09 MHz, CDCl<sub>3</sub>).

### Experiment 2:

[5][BF<sub>4</sub>] (0.002 mmol, 1.9 mg), TsNH<sub>2</sub> (0.1 mmol, 17.1 mg) and phenylacetylene (0.15 mmol, 16.5 μL) were mixed in CH<sub>2</sub>Cl<sub>2</sub> (0.3 mL) and CDCl<sub>3</sub> (0.3 mL). The mixture was transferred into an NMR tube which was capped and placed into an oil bath heated to 60 °C. After 3 h, the solution was analyzed by <sup>1</sup>H NMR spectroscopy. To collect the product, 4 mL of dry hexane was added to the reaction solution under vigorous stirring. The solution was then filtered and dried under vacuum overnight, giving imine **f** as a pale yellow solid (27.1 mg, ~99% yield). NMR spectroscopic data of **f** is consistent with literature precedents.<sup>4</sup> **<sup>1</sup>H NMR** (400.09 MHz, CDCl<sub>3</sub>): δ (ppm) 7.93 (d(m), <sup>3</sup>J<sub>H-H</sub> = 8 Hz, 2H, Ar<sub>tol</sub>-H), 7.90 (d(m), <sup>3</sup>J<sub>H-H</sub> = 8 Hz, 2H, Ar<sub>tol</sub>-H), 7.53 (tt, <sup>3</sup>J<sub>H-H</sub> = 8 Hz, <sup>4</sup>J<sub>H-H</sub> = 1 Hz, 1H, Ph-H), 7.41 (t(m), <sup>3</sup>J<sub>H-H</sub> = 8 Hz, 2H, Ph-H), 7.35 (d(m), <sup>3</sup>J<sub>H-H</sub> = 8 Hz, 2H, Ph-H), 2.99 (s, 3H, Me), 2.45 (s, 3H, Me). **<sup>13</sup>C{<sup>1</sup>H} NMR** (100.61 MHz, CDCl<sub>3</sub>): δ

(ppm) 180.0 (s), 143.6 (s), 138.8 (s), 137.7 (s), 133.3 (s), 129.6 (s), 128.7 (s), 128.4 (s), 127.2 (s), 21.7 (s), 21.3 (s).

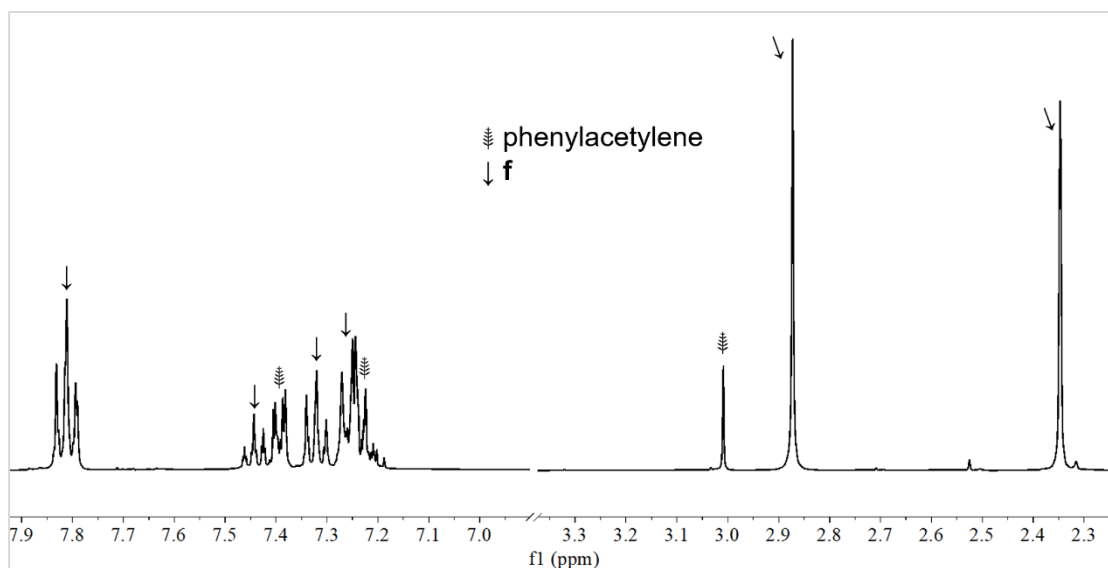


**Figure S39:** *In situ*  $^1\text{H}$  NMR spectrum of the hydroamination reaction of phenylacetylene catalyzed by [5][BF<sub>4</sub>] at 60 °C for 3 h (400.09 MHz, CDCl<sub>3</sub>).

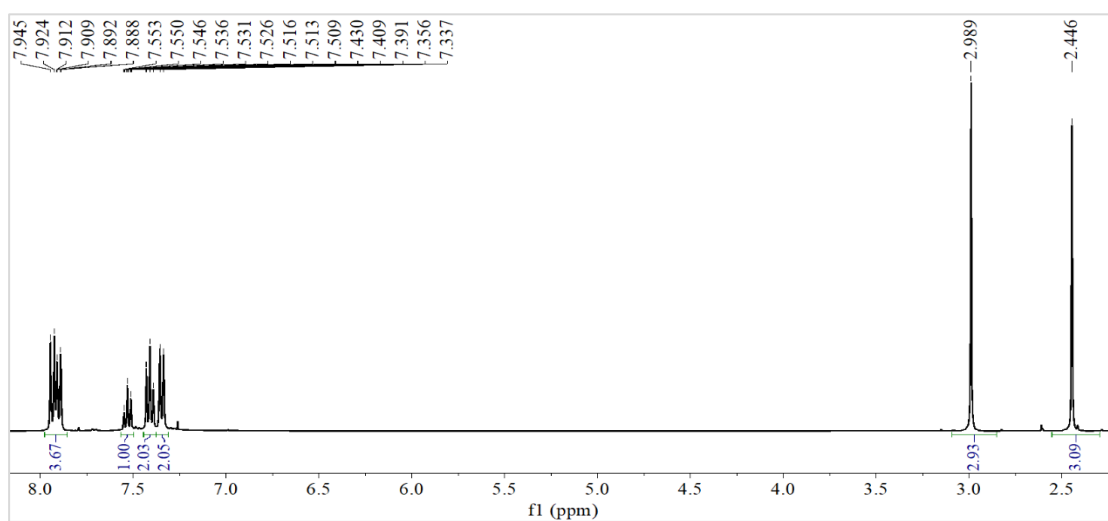


**Figure S40:**  $^1\text{H}$  NMR spectrum of isolated **f** (400.09 MHz, CDCl<sub>3</sub>).

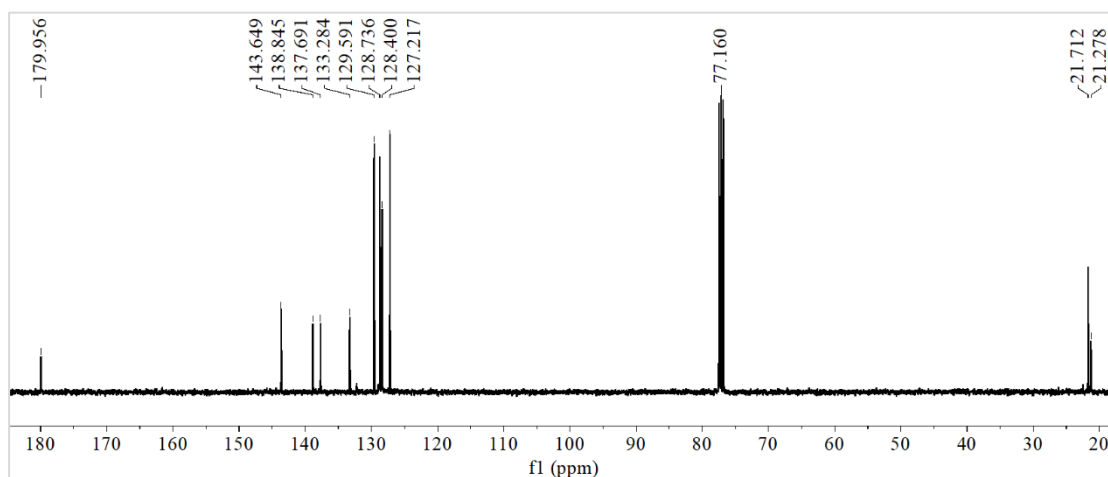


**Figure S41:**  $^{13}\text{C}\{^1\text{H}\}$  NMR spectrum of **f** (100.61 MHz,  $\text{CDCl}_3$ ).

### 2.2.2 Evaluation of $[\mathbf{3}]\text{BF}_4/\text{AgBF}_4$ as a catalyst

#### *Reaction 1: Cycloisomerization reaction of a:*

A stock solution of  $\text{AgBF}_4$  and  $[\mathbf{3}][\text{BF}_4]$  in  $\text{CDCl}_3$  (100  $\mu\text{L}$ , containing 0.0005 mmol of  $\text{AgBF}_4$  and 0.0005 mmol of  $[\mathbf{3}][\text{BF}_4]$ ) was added to an NMR tube containing **a** (0.1 mmol, 23.8 mg) in  $\text{CDCl}_3$  (0.5 mL). The reaction mixture was monitored *in situ* by  $^1\text{H}$  NMR spectroscopy at room temperature. No conversion was observed at the 10 min and 20 min time point.

#### *Reaction 2: Cyclization reaction of d.*

A stock solution of  $\text{AgBF}_4$  and  $[\mathbf{3}][\text{BF}_4]$  in  $\text{CDCl}_3$  (200  $\mu\text{L}$ , containing 0.001 mmol of  $\text{AgBF}_4$  and 0.001 mmol of  $[\mathbf{3}][\text{BF}_4]$ ) was added to an NMR tube containing **d** (0.1 mmol, 23.8 mg) in  $\text{CDCl}_3$  (0.4 mL). The reaction mixture was monitored *in situ* by  $^1\text{H}$  NMR spectroscopy at room temperature. No conversion was observed at the 10 min and 20 min time point.

#### *Reaction 3: Hydroamination reaction of phenylacetylene with p-toluenesulfonamide ( $\text{TsNH}_2$ ).*

A stock solution of  $\text{AgBF}_4$  and  $[\mathbf{3}][\text{BF}_4]$  in  $\text{CDCl}_3$  (100  $\mu\text{L}$ , containing 0.002 mmol of  $\text{AgBF}_4$  and 0.002 mmol of  $[\mathbf{3}][\text{BF}_4]$ ) was added to an NMR tube containing a mixture of  $\text{TsNH}_2$  (0.1 mmol, 17.1 mg) and phenylacetylene (0.15 mmol, 16.5  $\mu\text{L}$ ) in  $\text{CH}_2\text{Cl}_2$  (0.3 mL) and  $\text{CDCl}_3$  (0.2 mL). The tube was then capped and placed into an oil bath heated to 60  $^\circ\text{C}$ . After 2 h, the solution was analyzed by  $^1\text{H}$  NMR spectroscopy, showing 56% conversion.

### 3. Crystallographic Details

The crystallographic measurements were performed at 110(2) K using a Bruker APEX-II CCD area detector diffractometer (Mo-K $\alpha$  radiation,  $\lambda = 0.71069$  Å and Cu-K $\alpha$  radiation,  $\lambda = 1.54178$  Å). In each case, a specimen of suitable size and quality was selected and mounted onto a nylon loop. Semiempirical absorption corrections were applied. The structures were solved by direct methods, which successfully located most of the non-hydrogen atoms. Subsequent refinement using the SHELXTL/PC package (version 6.1) allowed location of the remaining non-hydrogen atoms which were refined anisotropically. H atoms (except H3 in [5][BF<sub>4</sub>]) were added at calculated positions using a riding model. Calculations were carried out using the SHELXL-2014 and Olex2 program.<sup>5</sup> The data has been deposited with the Cambridge Structural Database. CCDC 2076538 ([2][BF<sub>4</sub>]), 2076539 ([3][BF<sub>4</sub>]), 2076540 ([4][BF<sub>4</sub>]<sub>2</sub>) and 2076541 ([5][BF<sub>4</sub>]) contain the supplementary crystallographic data for this paper.

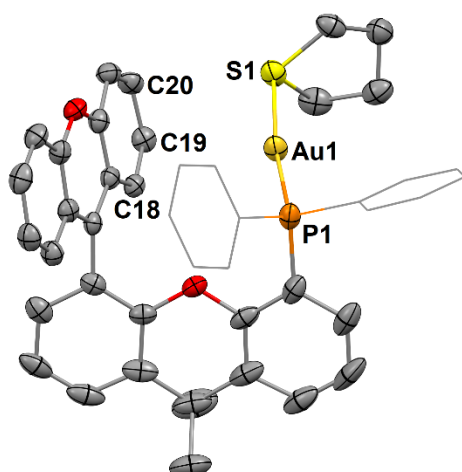


**Figure S42:** Structure of cation of [4][BF<sub>4</sub>]<sub>2</sub>. Counterions, solvent residues and hydrogen atoms omitted for clarity, thermal ellipsoids drawn at 50% probability, and phenyl groups drawn as thin lines.

#### 4. Computational Details

Starting from the solid-state geometry of  $[3][BF_4]$ , the structure of  $[3]^+$  was optimized using DFT methods as implemented in Gaussian 16.<sup>6</sup> These calculations were carried out with the BP86-D3(BJ) functional and the following mixed basis sets: Au SDD; P/Cl/C/O/H 6-31G\*. Frequency calculations found no imaginary frequencies. The structure of 4-xanthylium-9,9-dimethylxanthene ( $E^+$ ) was derived from the optimized structure of  $[3]^+$  and was generated by replacement of the “Ph<sub>2</sub>PAuCl” unit by a hydrogen atom which was placed in an idealized position using the GaussView 6 program<sup>7</sup> computationally. QTAIM calculations were carried out on the wave functions derived from the optimized structure using the AIMAll program.<sup>8</sup> NBO analysis was performed at using the NBO 6.0 program.<sup>9</sup> The NBO plot was visualized using Multiwfn<sup>10</sup> and VMD<sup>11</sup> (Visual Molecular Dynamics) programs. The electrostatic potential maps were visualized using GaussView 6 program.

##### NBO and AIM analysis of $[3]^+$

An atoms in molecules (AIM) analysis implemented at the optimized geometry of  $[3]^+$  reveals a bond path that connects these two atoms (**Figure S43**). The electron density value ( $\rho(r)$ ) of  $1.3 \times 10^{-2} \text{ e bohr}^{-3}$  at the corresponding bond critical point is low, speaking to the weakness of this interaction. A congruent picture emerges from natural bond orbital (NBO) calculations which shows the engagement of one of the chlorine electron pairs in a donor-acceptor interaction with a vacant NBO of  $\pi^*(C20-C21)$  parentage (**Figure S43**). This interaction is associated to a stabilization energy of  $3.3 \text{ kcal mol}^{-1}$  as indicated by a deletion calculation.

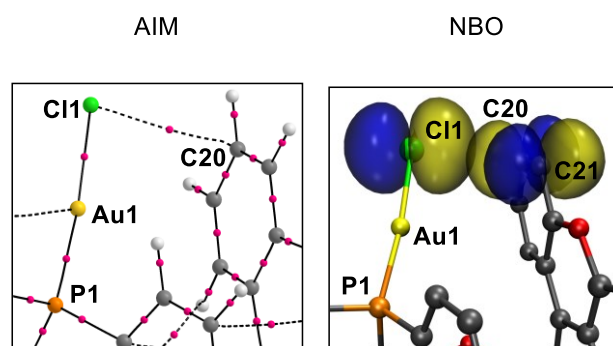


**Figure S43:** Left: AIM calculation results for  $[3]^+$  showing a bond path between Cl1 and C20. Right: NBO plot of the  $lp(Cl1) \rightarrow \pi^*(C20-C21)$  donor-acceptor interaction in  $[3]^+$  (isodensity value 0.04 a.u.).

**Cartesian coordinates for [3]<sup>+</sup> (in Å)**

C	0.072068	2.429109	0.272344
C	1.255497	1.908401	0.830452
C	2.173269	2.806288	1.408684
H	3.101119	2.423040	1.841920
C	-0.488663	-2.291901	-3.588398
H	0.058655	-2.724496	-4.428021
C	0.707591	4.667997	0.861987
H	0.512201	5.743516	0.876802
C	-0.799495	-0.902065	-3.593716
H	-0.465404	-0.285702	-4.431630
C	-0.903086	-3.111188	-2.539775
H	-0.703074	-4.185493	-2.528934
C	-2.149110	1.845684	-0.307890
C	-0.220321	3.802101	0.254843
C	-0.472150	-0.025312	2.632634
H	-0.424687	1.067712	2.680437
C	3.136114	-0.101970	1.701255
C	-3.092927	0.788206	-0.295372
C	-1.494092	-0.334197	-2.543932
H	-1.742234	0.728624	-2.553965
C	1.890408	4.178517	1.434790
H	2.600977	4.871913	1.894390
C	0.326724	-0.723631	1.706696
C	-4.878084	2.456260	-0.280635
H	-5.943900	2.702207	-0.283071
C	-2.699257	-0.631459	-0.353659
C	3.086089	-0.139773	3.110577
H	2.123327	-0.081319	3.629004
C	4.375818	-0.189092	1.034244
H	4.406640	-0.172616	-0.061626
C	-3.211303	-1.560472	0.608700
C	-4.580374	-2.158056	2.547682
H	-5.217040	-1.859458	3.385522
C	-4.025896	-1.190878	1.722596
H	-4.208054	-0.130170	1.907959
C	-1.626342	-2.535118	-1.488092
C	-4.469606	1.121168	-0.282281

H	-5.209015	0.315283	-0.313054
C	-1.458299	4.264924	-0.516943
C	-1.920793	-1.132173	-1.434419
C	4.273957	-0.260187	3.844659
H	4.235125	-0.294577	4.938311
C	-1.932229	5.662897	-0.082807
H	-2.217417	5.687978	0.982895
H	-2.794028	5.989499	-0.687799
H	-1.138839	6.408887	-0.251586
C	-1.328014	-2.140383	3.473900
H	-1.963542	-2.693760	4.171682
C	-0.548818	-2.835812	2.533587
H	-0.572504	-3.929805	2.501680
C	-4.312902	-3.532732	2.323061
H	-4.761294	-4.288544	2.975318
C	-2.543295	3.198454	-0.336554
C	-3.919188	3.481505	-0.305952
H	-4.253290	4.522175	-0.319637
C	-2.917469	-2.949793	0.451691
C	5.559959	-0.305797	1.776741
H	6.520669	-0.377508	1.257020
C	0.273638	-2.130787	1.644040
H	0.897862	-2.665522	0.918386
C	-3.464958	-3.932905	1.293458
H	-3.223140	-4.983254	1.110844
C	-1.300658	-0.737391	3.512607
H	-1.913910	-0.195773	4.240334
C	5.509422	-0.341899	3.179531
H	6.434361	-0.440066	3.757121
C	-1.083287	4.299406	-2.030858
H	-0.280130	5.036261	-2.203839
H	-1.962413	4.581825	-2.636105
H	-0.721646	3.315023	-2.375229
Au	1.915973	-0.643291	-1.387610
Cl	2.462429	-1.419350	-3.514918
P	1.611288	0.117768	0.716260
O	-2.106433	-3.394408	-0.544357
O	-0.814504	1.494514	-0.260780

**Cartesian coordinates for E<sup>+</sup> (in Å)**

C	-2.275934	0.709389	1.072768
C	-3.358952	1.602909	3.041847
H	-3.319411	2.187175	3.965182
C	2.399800	3.744606	-1.463500
H	2.630342	4.762925	-1.782149
C	-4.604327	0.257182	1.444628
H	-5.549313	-0.198974	1.137932
C	1.198785	3.123460	-1.910746
H	0.515540	3.686406	-2.550971
C	3.298672	3.056135	-0.650711
H	4.240638	3.501108	-0.320631
C	-0.964785	-0.534198	-0.458594
C	-3.467241	0.114106	0.628550
C	0.350482	-0.986078	-0.732611
C	0.888655	1.834820	-1.523173
H	-0.026149	1.355045	-1.875614
C	-4.553302	0.990696	2.638824
H	-5.452494	1.094933	3.253256
C	-0.610793	-2.843786	-1.995258
H	-0.479420	-3.740497	-2.607720
C	1.552119	-0.256358	-0.288315
C	2.588402	-0.942150	0.423863
C	3.593002	-2.936961	1.425173
H	3.518873	-3.987074	1.722238
C	2.504765	-2.305919	0.841073
H	1.567176	-2.843765	0.685219
C	2.990558	1.741841	-0.278303
C	0.505611	-2.157675	-1.513364
H	1.515284	-2.495032	-1.766095
C	-3.472068	-0.542977	-0.753719
C	1.770941	1.096627	-0.670824
C	-4.630474	-1.540992	-0.925393
H	-4.569710	-2.370421	-0.200108
H	-4.637180	-1.961473	-1.944477
H	-5.599821	-1.032705	-0.797075
C	4.797250	-2.224242	1.656581

H	5.652709	-2.733350	2.111273
C	-2.102313	-1.196956	-0.961557
C	-1.900730	-2.364089	-1.717401
H	-2.765417	-2.902700	-2.113657
C	3.796647	-0.242951	0.727949
C	4.897290	-0.873565	1.332710
H	5.804809	-0.293626	1.520158
C	-3.614066	0.592556	-1.813986
H	-4.578096	1.113331	-1.682163
H	-3.573330	0.170859	-2.833525
H	-2.807413	1.338852	-1.710355
O	3.950632	1.072278	0.421301
O	-1.089196	0.575708	0.353406
C	-2.195579	1.460239	2.261420
H	-1.273593	1.911087	2.564040

## 5. References

---

- <sup>1</sup> (a) L. Wang, M. Chen, P. Zhang, W. Li, J. Zhang, *J. Am. Chem. Soc.* **2018**, *140*, 3467-3473; (b) R. Uson, A. Laguna, M. Laguna, D. A. Briggs, H. H. Murray, J. P. Fackler Jr., *Inorganic Syntheses*, **1989**, 85-91.
- <sup>2</sup> Y. Tang, B. Yu, *RSC Adv.* **2012**, *2*, 12686-12689
- <sup>3</sup> E. D. Litle, L. C. Wilkins, F. P. Gabbaï, *Chem. Sci.* **2021**, *12*, 3929.
- <sup>4</sup> Q. Yang, G. Shang, W. Gao, J. Deng, X. Zhang, *Angew. Chem. Int. Ed.* **2006**, *45*, 3832-3835.
- <sup>5</sup> (a) G. M. Sheldrick, *SADABS, An Empirical Absorption Correction Program for Area Detector Data*; University of Göttingen, Göttingen, Germany, 1996; (b) G. M. Sheldrick, *SHELXL-2014*, University of Göttingen, Göttingen, German, 2014; (c) Bruker, 2019, *APEX3 (v2019.2011-2010)*, Bruker AXS Inc., Madison, Wisconsin, USA; (d) O. V. Dolomanov, L. J. Bourhis, R. J. Gildea, J. A. K. Howard and H. Puschmann, *OLEX2: a complete structure solution, refinement and analysis program*, *J. Appl. Cryst.*, 2009, **42**, 339-341
- <sup>6</sup> M. J. Frisch, G. W. Trucks, H. B. Schlegel, G. E. Scuseria, M. A. Robb, J. R. Cheeseman, G. Scalmani, V. Barone, G. A. Petersson, H. Nakatsuji, X. Li, M. Caricato, A. V. Marenich, J. Bloino, B. G. Janesko, R. Gomperts, B. Mennucci, H. P. Hratchian, J. V. Ortiz, A. F. Izmaylov, J. L. Sonnenberg, D. Williams-Young, F. Ding, F. Lipparini, F. Egidi, J. Goings, B. Peng, A. Petrone, T. Henderson, D. Ranasinghe, V. G. Zakrzewski, J. Gao, N. Rega, G. Zheng, W. Liang, M. Hada, M. Ehara, K. Toyota, R. Fukuda, J. Hasegawa, M. Ishida, T. Nakajima, Y. Honda, O. Kitao, H. Nakai, T. Vreven, K. Throssell, J. A. Montgomery, Jr., J. E. Peralta, F. Ogliaro, M. J. Bearpark, J. J. Heyd, E. N. Brothers, K. N. Kudin, V. N. Staroverov, T. A. Keith, R. Kobayashi, J. Normand, K. Raghavachari, A. P. Rendell, J. C. Burant, S. S. Iyengar, J. Tomasi, M. Cossi, J. M. Millam, M. Klene, C. Adamo, R. Cammi, J. W. Ochterski, R. L. Martin, K. Morokuma, O. Farkas, J. B. Foresman, and D. J. Fox, Gaussian, Inc., Wallingford CT, 2016.
- <sup>7</sup> GaussView, Version 6, Roy Dennington, Todd A. Keith, John M. Millam, Semichem Inc., Shawnee Mission, KS, **2016**.
- <sup>8</sup> AIMAll (Version 19.02.13), Todd A. Keith, TK Gristmill Software, Overland Park KS, USA, 2019 (aim.tkgristmill.com).
- <sup>9</sup> E. D. Glendening, J. K. Badenhoop, A. E. Reed, J. E. Carpenter, J. A. Bohmann, C. M. Morales, F. Weinhold, Theoretical Chemistry Institute; University of Wisconsin: Madison, WI, 2009.
- <sup>10</sup> T. Lu, F. Chen, *J. Comput. Chem.* **2012**, *33*, 580-592.
- <sup>11</sup> W. Humphrey, A. Dalke, K. Schulten, *J. Molec. Graphics* **1996**, *14*, 33-38.